Review

Recent research progress of bismuth-based electrocatalysts for electrochemical reduction of carbon dioxide

Chen Zhang[1], Fei Liu[1], Jia-Jun Wang[1], Guang-Jin Wang[2], Zhao-Yong Sun[5], Qiang Chen[5], Xiao-Peng Han[1], Yi-Da Deng[3], Wen-Bin Hu[1,4]

[1]Key Laboratory of Advanced Ceramics and Machining Technology of Ministry of Education, School of Materials Science and Engineering, Tianjin University, Tianjin 300072, China.
[2]School of Materials Science and Hydrogen Energy, Foshan University, Foshan 528000, Guangdong, China.
[3]State Key Laboratory of Marine Resource Utilization in South China Sea, School of Materials Science and Engineering, Hainan University, Haikou 570228, Hainan, China.
[4]Joint School of National University of Singapore and Tianjin University, International Campus of Tianjin University, Fuzhou 350207, Fujian, China.
[5]China Energy Lithium Co., Ltd, Tianjin 300072, China.

Correspondence to: Prof. Jia-Jun Wang, Key Laboratory of Advanced Ceramics and Machining Technology of Ministry of Education, School of Materials Science and Engineering, Tianjin University, 135 Yaguan Road, Tianjin 300072, China. E-mail: wangjiajun90@tju.edu.cn; Prof. Guang-Jin Wang, School of Materials Science and Hydrogen Energy, Foshan University, 18 Jiangwan Road, Foshan 528000, Guangdong, China. E-mail: wgj501@163.com

Abstract

With modern science and technology developing, the concentration of atmospheric carbon oxide (CO_2) has increased substantially. CO_2 electroreduction reaction (CO_2RR) can efficiently utilize sustainable power to produce value-added chemicals and implement energy storage. Previous researches have proved bismuth metal and bismuth-based materials can transfer CO_2 to formate selectively. However, in this paper, the latest progress in the synthesis of advanced electrocatalysts with bismuth-based CO_2RR catalysts is reviewed from the aspects of catalyst material design, synthesis, reaction mechanism and performance verification/optimization. Some methods of designing catalysts are discussed and analyzed from different angles, including catalyst morphology, defects and heterogeneous structures. In particular, the application of *in situ* characterization technique in catalyst characterization is introduced. Subsequently, some views and expectations regarding the current challenges and future potential of CO_2RR research are presented.

Keywords: Bismuth-based catalysts, CO_2RR, *in situ* characterization technique, formate, reconstruction

INTRODUCTION

With the overuse of fossil fuels since the industrial revolution, the rapidly rising level of carbon dioxide (CO_2) in the atmosphere has facilitated the development of various strategies for converting carbon dioxide into valuable chemical products and maintaining the dynamic balance of the carbon cycle in nature. At present, there are many kinds of artificial conversion technologies, mainly including electroreduction, bioconversion, photoreduction, and thermal conversion. Among all these techniques, electrocatalytic CO_2 reduction reaction (CO_2RR) is currently receiving much attention due to its various advantages such as mild reaction conditions, recyclable electrolytes, and environmentally friendly driving force for potential synergies with renewable electricity. At the same time, CO_2RR can take full advantage of the carbon dioxide to produce many industrial facilities and effectively achieve carbon reduction goals[1-6]. Due to the diversity of catalysts and reaction environments, CO_2RR products are also very diverse, which can produce many valuable chemical products. Examples include one-carbon products such as carbon monoxide (CO)[7], methane (CH_4)[8,9], formic acid ($HCOOH$) or formate ($HCOO^-$)[10,11], methanol (CH_3OH)[12,13], and already multi-carbon products such as ethylene (C_2H_4)[14,15], ethanol (CH_3CH_2OH)[16,17], n-propanol (n-C_3H_7OH)[18,19], *etc.* (The different reaction paths are shown in Table 1). Over the past few decades, a large amount of research from catalyst design[20-22] to electrolyte regulation[23,24] and device engineering have made great efforts on developing and boosting CO_2RR to yield carbon-based products. However, there are still many challenges for CO_2RR to consider and solve. Firstly, carbon dioxide is a linear molecule with π bonds, and its reduction involves geometric changes in the geometric shape of the linear molecule. Therefore, it has an enormous reorganization and activation energy. Without any catalyst, the first step of electron transfer is to form free intermediate $^*CO_2$. In this reaction, the $^*CO_2$ intermediate was formed at the catalytic surface at -1.9 V (*vs.* standard hydrogen electrode, or RHE)[25,26]. Furthermore, due to the complexity and diversity of the catalytic reaction pathways, involving a variety of electron transfer pathways and proton participation, the reduction product selectivity is limited. In addition, many competitive reactions will also affect the catalytic efficiency of CO_2RR. For example, the hydrogen evolution reaction (HER) will seriously affect the CO_2 conversion efficiency by reason of its close potential with the CO_2RR[27]. Therefore, the selection of a CO_2RR catalyst system has become the focus of current research.

Bismuth (Bi), with atomic number 83, located in the sixth period of Group VA of the periodic table, is a typical semi-metallic element with covalent bonds. In nature, a small portion exists in free form, since a large fraction exists in compound form[28,29]. The features of bismuth include affordability, environmental friendliness and nontoxicity. The cost of bismuth is much lower than the price of indium, a common CO_2RR catalyst, and comparable to the price of tin. Bismuth metal has a layered crystal structure similar to black phosphorus. It can be peeled into two-dimensional (2D) monolayers or multilayers, and this lamellar structure expands the specific surface area[30]. In addition, bismuth has a highly reversible redox reaction and a suitable voltage window in aqueous solution, which is vastly used in electrocatalysis, energy storage, environmental protection, photocatalysis and many other domains. Many studies have shown that many P-zone metallic elements have favorable electronic structures and favorable reduction of CO_2 to formate[31]. Although Hg, Cd, Pb, Tl and other heavy metals can convert CO_2 into formate, the high poisonousness and cost of these heavy metals limit the development for CO_2RR[32]. On account of its unique structure of weak bonding ability towards $^*HCOO$, nontoxicity, and inhibition of HER generation, Bi and Bi-derived catalysts have so far aroused tremendous attention for CO_2RR to formate. The application of Bi metal in CO_2RR was first introduced by Komatsu *et al.* in 1995[33]. However, it did not receive as much attention as Sn did in the early days. Prior to 2016, Bi produced CO mainly through CO_2RR in ionic liquids or aprotic electrolytes. Recently, the great potential of Bi to selectively generate formate through CO_2RR in aqueous solutions has been explored and systematically reviewed[34,35]. Bismuth has a low melting point and oxidizes easily in air.

Table 1. Different products, pathways and reaction potentials of CO_2RR[36]

Product	Reaction	E_0/V (*vs.* RHE)
Activation	$CO_2 + e^- \rightarrow {}^*COO^-$	-1.90
HCOOH	$CO_2 + 2H^+ + 2e^- \rightarrow HCOOH$	-0.55
CO	$CO_2 + 2H^+ + 2e^- \rightarrow CO + H_2O$	-0.52
CH_3OH	$CO_2 + 6H^+ + 6e^- \rightarrow CH_3OH + H_2O$	-0.38
CH_4	$CO_2 + 8H^+ + 8e^- \rightarrow CH_4 + 2H_2O$	-0.24
C_2H_4	$2CO_2 + 12H^+ + 12e^- \rightarrow C_2H_4 + 4H_2O$	-0.38
CH_3CH_2OH	$2CO_2 + 12H^+ + 12e^- \rightarrow CH_3CH_2OH + 3H_2O$	-0.35
C_2H_6	$2CO_2 + 14H^+ + 14e^- \rightarrow C_2H_6 + 4H_2O$	-0.28
C_3H_7OH	$3CO_2 + 18H^+ + 18e^- \rightarrow C_3H_7OH + 5H_2O$	-0.30
CH_3OH	$CO_2 + 6H^+ + 6e^- \rightarrow CH_3OH + H_2O$	-0.38
H_2	$2H^+ + 2e^- \rightarrow H_2$	0

Therefore, its nanostructures are chemically unstable. The rational design of nanostructured electrocatalysts should not only enlarge its surface area, but also improve its actual activity and catalytic stability. By introducing structural perturbations or defects in the electrocatalyst, the electronic states can be modulated. At the same time, more incongruity and highly active sites are produced. In addition, by some modification strategies, such as transforming the defective bismuth compound, it is possible to construct bismuth nanostructures rich in defects to achieve the above goals. The structure and performance of the actual Bi-based electrocatalyst can be optimized by cutting the structure of the initial template. However, the Bi-based catalyst performed well in the CO_2RR. There are still many challenges and problems to be solved for further commercial applications in formate systems: (1) Although some excellent Bi-based catalysts have achieved good activity for CO_2RR, whose performance does not meet industry standards; (2) Structural/compositional reconfiguration during operation leads to decreased stability and selectivity; (3) The real active site and catalytic mechanism of the dynamic catalytic process are still difficult to reveal.

Based on the above consideration, the exploration of efficient Bi and Bi-based CO_2RR catalysts with good activity and selectivity can achieve sustainable utilization of energy. Meanwhile, it is significant to fundamentally understand the mechanism of action of different catalytic sites, which will help design optimal catalysts with satisfactory CO_2RR activation effects. In recent years, many reviews of CO_2RR electroreduction reactions have been reported. There have been many instructive reviews on CO_2RR. Han *et al.* reviewed the research of main group metal elements such as tin, bismuth and indium in CO_2RR, and summarized the catalyst modification strategy and application in flow and membrane electrode assembly (MEA) cells[36]. Similarly, Li *et al.* also discuss the main group metal elements and review the research progress from different nanostructures and synthesis strategies[37]. Guan *et al.* introduced the application of Bi elements in CO_2RR from the perspective of electrolyte and different nano-morphology engineering[38]. Xia *et al.* reviewed the Bi and BiSn binary system, especially the research progress in solid electrolytes in flow cells[39]. There are many related studies on the key remodeling process of Bi elements in the catalytic process, but few reviews summarize the mechanism of this aspect. In addition, it is difficult to capture key information about intermediates and gain a deep understanding of the reaction mechanism. Therefore, increasing *in situ* techniques are used for CO_2RR. However, the relevant reviews in this area are still insufficient. In this mini-review, we report the up-to-date work of Bi-based CO_2RR catalysts in recent years. We specifically pay more attention to Bi and Bi-based compounds and modification strategies for formate and other products. First of all, we generally discuss the fundamental reaction mechanism of CO_2RR; particularly, we introduce the importance of reconstruction for CO_2RR. Then, we introduce the recent progress of various modified strategies of Bi-based catalysts to improve the performance of CO_2RR in detail;

especially, the role of the reconstruction process and density functional theoretical (DFT) calculation in each work is highlighted. In addition, we systematically summarize the role and application of various *in situ* instruments in CO_2RR in recent studies, especially for the monitoring of *in situ* instruments in Bi-based catalysts. Finally, the advantages of Bi and Bi-based catalysts are summarized, and the future development direction is discussed. And the application of more advanced characterization techniques such as optimal design, mechanism interpretation, *in situ* characterization techniques and the improvement of electrochemical reaction equipment are also highlighted. In this review, the advantages of Bi-based catalysts are analyzed from the structural characteristics and reaction paths of Bi-based catalysts, and the process of reconfiguration is explained by *in situ* characterization technology. This mini-review will pave the way for exploring new high-performance catalysts to obtain the desired products from CO_2RR.

ELECTROCHEMICAL CATALYTIC REDUCTION OF CARBON DIOXIDE AND RECONSTRUCTION PROCESS

First, we briefly introduce the CO_2RR with the formic acid reaction process and reaction path. These pathways rely on adsorbed intermediates on the electrode surface, such as *COOH, *OCHO, and *H. Because CO_2 is a relatively inert molecule, the first process of electron transfer to a CO_2 adsorption surface to form a CO_2 intermediate is generally considered to be the rate-determining step of the CO_2RR[40]. The manner in which the activated $*CO_2 \cdot^-$ binds to the electrode surface plays a decisive role to the next protonation step. $*CO_2 \cdot^-$ binds to forms *COOH through the combining carbon atoms on the electrode. In addition, formic acid formation by *H adsorption has also been suggested as a possible reaction pathway[41]. Selectivity in the CO_2RR process is mainly determined by the relative bonding strength of the reaction intermediates [*COOH, *OCHO, *CO, and *H (intermediates of H_2)] at the electrode surface. Due to its oxophilicity, Bi tends to form carbon-oxygen bond intermediates such as *OCHO rather than *COOH[42]. In addition, the dioxygen-bonded intermediates are more stable than single-bonded intermediates[43]. Therefore, the binding energy of *COOH [Figure 1A] and *H [Figure 1B] on Bi surfaces is higher than that of *OCHO [Figure 1C], which is widely considered as the most practicable reaction pathway[37]. Table 1 displays the different CO_2RR pathways according to the number of electron transfers. Since the same two electrons are transferred, CO is also produced apart from formic acid. This is due to the fact that CO is produced along this path when the material and the environment are favorable for the adsorption intermediate *OCHO. Figure 2 shows the relationship between the adsorption energies of different metals for distinct intermediates in CO_2RR and their products[43]. The higher adsorption energy of *CO and *H will generally form the two-electron transfer product of CO and formic acid.

Reconstruction of an electrocatalyst refers to any change in the chemical composition and/or structure of its surface or its whole bulk and it is widely observed in chemical reactions[44-46]. In addition, according to the scale and principle of reconstruction, it can be categorized into topological, chemical and crystal reconstructions. It is supposed that these are main factors that can lead to the reconfiguration of the precatalyst: the deviation pressure applied during catalysis and the variable test conditions. In such molecular conversion catalysis, the potential required for experimental manipulation of the catalyst material is usually more correct or negative than the equilibrium potential. If the applied potential exceeds the reduction and oxidation potential of the elements contained in the material, it may lead to precatalyst instability and changes in the surface valence states[47]. If this process is irreversible upon potential recovery, then this evolution continues, eventually producing a reconstructed layer of new species and forming a core-shell structure. In CO_2RR, when the potential of activation and reduction of CO_2 is very negative, the valence of the metal compound cannot be maintained, and the precatalyst will undergo reduction reaction to become metal, which is the real substance that plays a catalytic role[48,49].
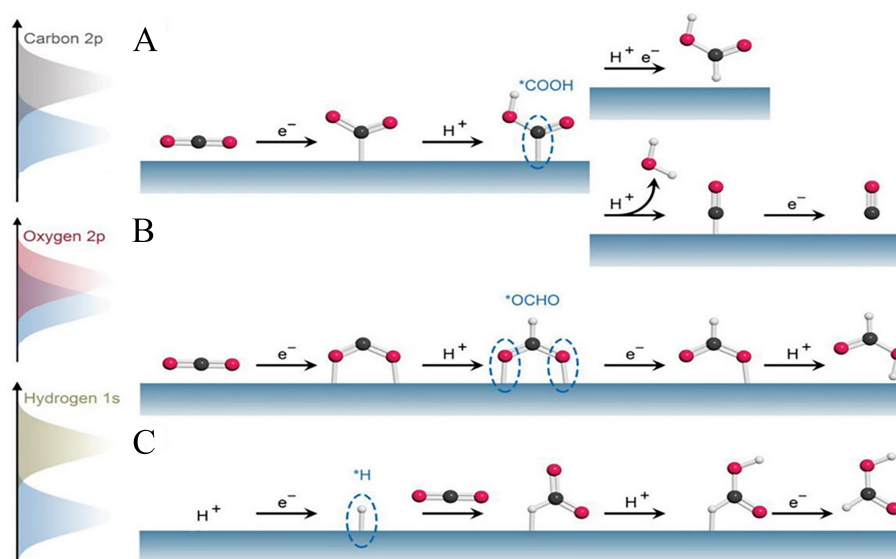
Figure 1. Schematic diagram of different reaction pathways of CO_2RR to formic acid through the formation of different intermediates. (A) *COOH intermediate adsorbed on the catalyst surface via carbon atom; (B) *OCHO intermediate adsorbed on the catalyst surface via oxygen atom; (C) *H intermediate adsorbed on the catalyst surface via hydrogen atom (color code: C, black; O, red; H, white). Reprinted with permission from Ref.[37]. Copyright 2023, Wiley-VCH.

The reconfiguration process is significant for catalysis and has many advantages[49]: (1) There are often abundant vacancies/defects, active sites or coordination of unsaturated metal atoms after reconstruction; (2) A large part of the reason for the reconstruction of the multi-empty nano-catalytic structure is due to the precipitation of components, thus forming a porous and multi-defect structure, which can promote the effective transmission of the solution and the diffusion of the gas. At the same time, this transport structure can also avoid the reduction of catalyst activity caused by agglomeration in the catalytic process; (3) Since the reconstructed product is more thermodynamically stable than the precatalyst, the fully reconstructed catalyst is expected to show high catalytic/component stability; (4) The doping uniformity can be adjusted, which is more conducive to the control of electronic structure. In particular, during the CO_2RR, negative reduction potentials lead to the surface reconstruction of Bi-based compounds into metallic Bi^0, which will also have a very important impact on the subsequent catalytic activities as the active phase[50,51].

THE RESEARCH PROGRESS OF BI METAL-BASED ELECTROCATALYSTS

Due to the adjustability of size and morphology, effectively using size effect to improve CRR performance has become a hot spot for researchers to explore. Adjusting the adsorption energy between the active sites and the intermediates via the size effect can greatly affect the reaction pathway and the efficiency of the product. However, the dependence of CO_2 reduction on Bi size has been rarely explored due to the fundamentally different nature of catalytic properties. Major challenges include: (1) difficulty in achieving uniform distribution of bimetallic sites of different sizes, (2) unclear interaction between metal and matrix, and (3) low melting points leading to solid structure collapse and solid oxidation during the reaction. So far, Bi-based electrocatalysts used in the CO_2RR field have been customized with different morphologies characteristics [such as single-atom catalysts (SAC), nanoparticles, one-dimensional nanowires (NW) and nanotubes (NT), 2D nanosheets, nanomembranes, nano-dendrites, *etc.*][38]. And these various types of catalysts can be prepared by various ways including hydrothermal methods, chemical reduction, electroreduction, electrodeposition, and so on. The Bi-based catalyst produced formate from CO_2 in aqueous solution, which has the characteristics of high efficiency, good selectivity and great stability. Designing ,preparing and characterizing Bi-based catalysts with increasing Faraday efficiency (FE) will
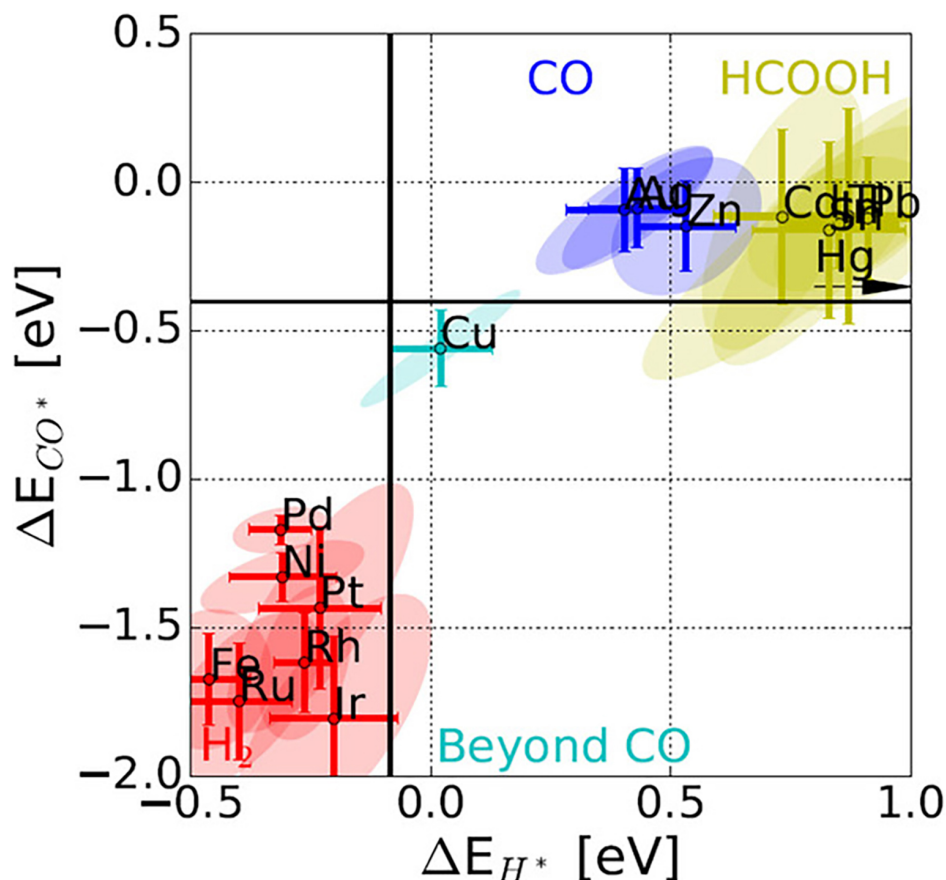
Figure 2. The binding energies of the intermediates $*\Delta E_{CO}$ and $*\Delta E_H$ can be used to separate the Cu metal catalyst into its own group and, hence, explain the beyond $*CO$ group. Where the beyond $*CO$ group bind to $*CO$ while not having H_{upd}. Reprinted with permission from Ref.[43]. Copyright 2017, Wiley-VCH.

provide more specific research directions for improving performance. The environment of Bi atoms will directly affect the catalytic products and catalytic efficiency. This section mainly reports the latest research progress of Bi elements and Bi atoms in CO_2RR, and analyzes the influence of different forms on Bi catalysis.

Single-atom catalysts

Recent studies have indicated that nanometallic materials have better competence in CO_2RR than bulk materials due to their higher specific surface area and size effects. Therefore, expanding their specific area through nanoscale structural engineering is very important to improve their catalytic performance. SAC, as an attractive heterogeneous catalyst, shows unique advantages in electrocatalysis. SAC has tremendous advantages as follows over the traditional nanocatalysts: i) Substantially higher atom utilization, even up to 100%: as the particle size of catalyst is reduced, the atom dispersion is continuously improved until it reaches complete dispersion, resulting in exposing more active catalytic sites and thus significantly boost catalytic performance; ii) Regulable coordination environment: the coordination number and coordination atoms of the metal catalytic sites dispersed on various carriers are often adjustable, so as to regulate unsaturated and supersaturated coordination structures to obtain unprecedented catalytic performance; iii) Metal-carrier interaction: in SAC, there is strong mutual anchoring between isolated catalytic atoms and carriers and this interaction is beneficial to electron transfer, which can not only structurally prevent metal atoms from flocking together into clusters, but also facilitate the formation of strong chemical bonds

between metals and carriers[52]. For CO_2RR, well-defined active centers in SAC have the potential to reduce the diversity of reaction pathways or weaken HER. Applying SAC in the field of CO_2RR to regulate product distribution makes sense, both in terms of productivity and cost savings. In most cases, due to the unsaturated coordination structure, the central atom that provides a suitable adsorption/desorption site for the reaction intermediate acts as the active center. Sometimes, the reconfiguration of SAC occurs during the catalytic process, resulting in a change in the active component SAC to the nanoparticle/cluster. The reasonable construction of the coordination structure gives SAC an incomparable advantage in electrocatalytic CO_2 reduction.

Zhang *et al.* used Bi-based metal-organic framework (MOF) precursors to obtain Bi SAC immobilized on porous carbon supports [Figure 3A][53]. They effectively used *in situ* environmental transmission electron microscopy (ETEM) to monitor the catalytic process of the catalyst. The Bi-based MOF precatalyst was reconstructed to single Bi atoms riveted on N-doped carbon networks (Bi SAC/NC). DFT calculations indicate that $Bi-N_4$ as the active center of the Bi SAC/NC catalyst optimized the catalytic activity by reducing the energy barrier for the formation of *COOH intermediate [Figure 3B]. The atomically distributed catalytic site changes the adsorption energy of *COOH and *CO, making CO more selective than formic acid.

The Bi SAC in different coordination environments also shows different selectivity of CO_2RR products. Santra *et al.* synthesized atomically dispersed Bi SAC with carbon black as a carrier[54]. Scanning transmission electron microscopy (STEM) and extended X-ray adsorption fine structure (EXAFS) studies have confirmed the success of monatomic morphology synthesis at low and high temperature annealing [Figure 3C]. The SAC coordination environment in the carbon-nitrogen framework was significantly changed by changing the synthesis parameters under high temperature and low temperature treatment. The low temperature treatment resulted in a high load of the Bi_2O_3 coordination center, while the high temperature treatment resulted in low coverage of the Bi_2N site [Figure 3D]. The spectra show that under the same electrochemical CO_2RR conditions, nitrogen-coordinated Bi SAC tends to produce CO, while oxygen-coordinated Bi SAC mainly generates HCOOH.

Furthermore, the single atom alloy (SAA) catalyst composed of single atoms of Bi and other isolated atoms of external metals has recently received extensive attention as a special SAC. Monatomic alloys have the following main advantages: i) The structure of the active center of SAA is determined, which facilitates the understanding of the relationship between the structure of catalyst and performance[55,56]; ii) SAA catalysts may exhibit particular electronic structures and strong synergies among different metals, thus breaking the linear scaling used to promote heterogeneous catalytic activity and/or selectivity[57,58]; The early development of SAA catalyst was mainly to optimize the performance during the process of multiphase thermal catalysis, and recently, the application field of SAA catalyst has been expanded to photocatalysis and electrocatalysis, demonstrating its rationality in adjusting electronic structure and various multiphase catalytic properties.

BiCu-SAA was synthesized *in situ* by electrochemistry using Bi-CuS precursors [Figure 4A][59]. The catalyst can promote C-C coupling in the catalytic process, and the addition of copper improves the selectivity of electrocatalytic CO_2RR to generate C_{2+} products, and 73.4% of high C_2 products can be obtained at -0.9 $V_{vs RHE}$. At a high current density of 400 mA·cm^{-2}, the developed BiCu-SAA catalyst also maintained its structural stability and showed good robustness [Figure 4B]. *In situ* Fourier-transform infrared spectroscopy (FTIR) based on Synchrotron radiation (SR-FTIRs) showed that the peak intensity of BiCu-SAA was significantly higher than that of Cu-nano-samples, indicating that the BiCu-SAA catalyst had better *CO generation ability [Figure 4C]. DFT calculations show that the position of the Bi state below the Fermi level
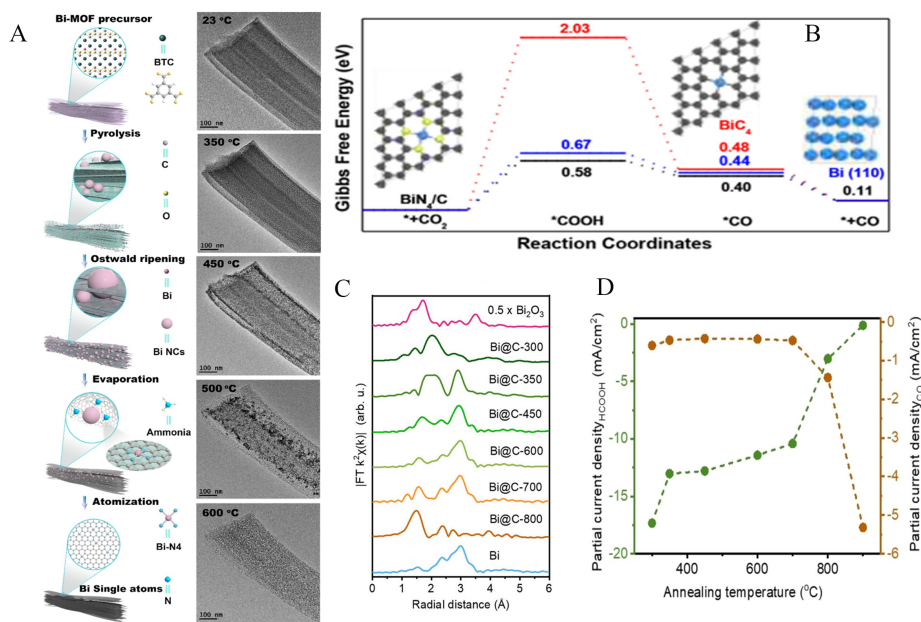
Figure 3. (A) Diagram of the transformation to Bi SACs and TEM images of Bi-MOF decomposed at different reaction temperatures; (B) DFT diagrams for CO$_2$RR on different catalysts. Reprinted with permission from Ref.[53].Copyright 2019, American Chemical Society; (C) The EXAFS spectra from Bi L$_3$ edge XANES spectra of Bi@C samples annealed at different temperatures, along with Bi foil and Bi$_2$O$_3$ as references; (D) Electrochemical testing of CO$_2$RR products HCOOH and CO as a function of annealing temperatures for Bi@C catalysts. Reprinted with permission from Ref.[54].Copyright 2023, Wiley-VCH. SAC: Single-atom catalysts; TEM: transmission electron microscopy; MOF: metal-organic framework; DFT: density functional theory; EXAFS: extended X-ray adsorption fine structure; XANES: X-ray absorption near edge structure.
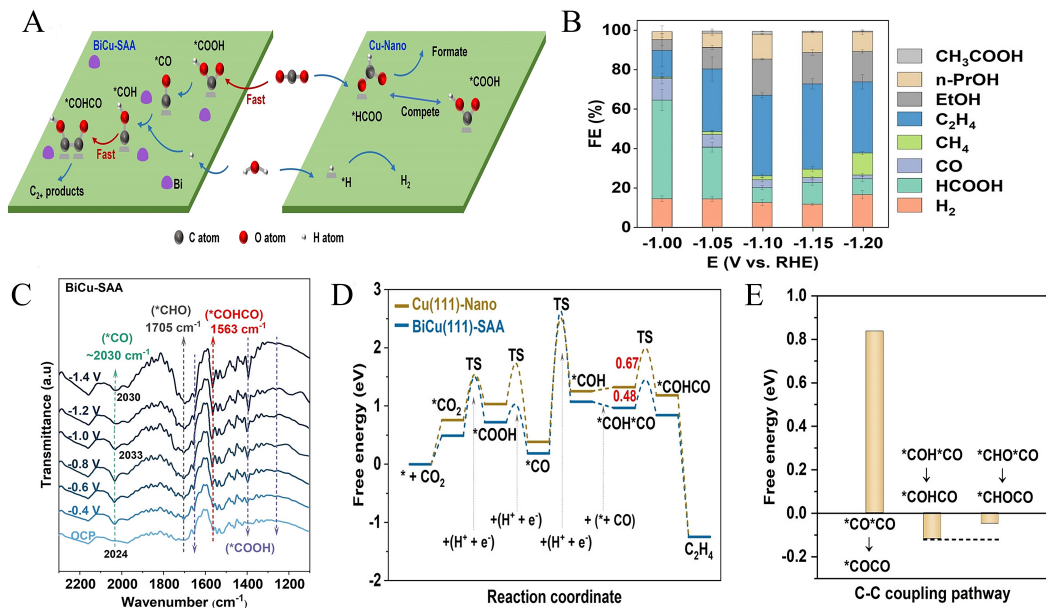
Figure 4. (A) The supposed reaction mechanism of CO$_2$RR on the BiCu (111)-SAA (left) and Cu (111)-Nano (right); (B) FE values of different products; (C) *In situ* SR-FTIR spectra of BiCu SAA and Cu nanocatalyst at different potentials; (D) DFT diagram for the CO$_2$RR to C$_2$H$_4$ on the surface of catalysts; (E) The free energy plots for different processes. Reprinted with permission from Ref.[59]. Copyright 2023, Wiley-VCH. SAA: Single atom alloy; FE: faraday efficiency; FTIR: fourier-transform infrared spectroscopy; DFT: density functional theory.

in the projected density of states (PDOS) results proves that the Bi site acts as a promoter/modifier to change the electronic structure of the copper plate. The localized electrons can be transferred to the antibonding orbital of the CO_2 molecule. Through the analysis of the reconstruction process, unlike most series catalysts, this catalyst mainly reduces the energy of CO_2 adsorption/activation by optimizing the electronic structure of metal nanoparticles. BiCu-SAA catalyst can achieve rapid consumption of *CO intermediates, so as to achieve the purpose of optimization of intermediates [Figure 4D and E]. Moreover, with the single Bi-SAC and Cu-SAC, the optimization of catalytic products and the stability of catalytic process can be realized, and the purpose of one plus one is greater than two is realized. It is well known that SAC can be used as a model system to fundamentally understand the CO_2RR mechanism in terms of the active site as well as the interaction between atomically dispersed metal catalysts and supporting materials. However, this is necessarily accompanied by difficulties of the SAC itself, including scale-up synthesis and atomic-level characterization of high metal loading, identification of active sites, and understanding of basic mechanisms.

1D nanostructures

One-dimensional nanomaterials, such as NW (including alloys and coaxial heterostructures) and NT[60], are considered as active and stable electrode contact regions for electronic materials due to their distinct and homogeneous structure, easy electron transfer, shortened ion diffusion distance, increased electrolyte, and rigid durability corresponding to unidirectional stress and strain[61]. Due to the strong boundary effect and the quantum binding principle, the abundant open Spaces and pores between adjacent one-dimensional nanostructures enable the rapid transfer and reaction of catalyst molecules on the electrode/catalyst surface. Therefore, one-dimensional nanomaterials are supposed to be an excellent electrochemical catalysis[33].

Zhang *et al.* reported a strategy of lattice dislocation Bi NW (Cu@BiNW) on the surface of copper foam by *in situ* electrochemical preparation of Bi atoms[62]. The electrochemical test data show that Cu@BiNW is a high efficiency electrocatalyst with low overpotential, a FE of 95%, and a formic acid current density of about 15 mA·cm^{-2}. Compared with RHE, the FE formate value remains above 93% in the voltage range of 0.69-0.99 $V_{vs RHE}$. Fourier transform alternating current (AC) voltammetry studies showed significant differences in the catalytic path and rate compared to other Bi-based materials. Due to the high porosity, the catalytic surface area is significantly improved. At the same time, due to the introduction of a considerable number of lattice dislocations in the Bi NW, the CO_2 reduction activity of the Cu@BiNW electrode is greatly enhanced.

2D nanosheets

Due to the excellent properties of layered graphene in many aspects, 2D single crystals are also currently being investigated. Bismuth is the largest atomic mass member of group VA in 2D elemental crystals and has a quasi-layered structure similar to that of rhombic antimony and arsenic. Ultra-thin Bi nanosheets are effective CO_2RR electrocatalysts with significant FE and high current density. Despite its many excellent physical and electrical properties, experimental realization of single-crystal 2D bismuth has been hindered.

Zhang *et al.* used the liquid phase dissolution method to dissolve powder Bi in isopropanol (IPA) solution of NaOH by ultrasonic, and prepared ultra-thin Bi nanosheets on a large scale [Figure 5A][63]. The successful synthesis of Bi nanosheets was confirmed by high-resolution transmission electron microscopy (HETEM), Raman and ultraviolet (UV)-visible spectroscopy. Bi nanosheets offer several advantages, including their ultra-thin structure, high electron transfer rate, good CO_2 adsorption rate, and high electrical conductivity. They also showed that Bi nanosheet edges with more catalytic sites can effectively promote the generation of *OCOH, a key intermediate for CO_2 selective production of formic acid. DFT calculations indicate that *OCOH intermediates tend to form at the margin positions of Bi nanosheets to reconstruct a more stable
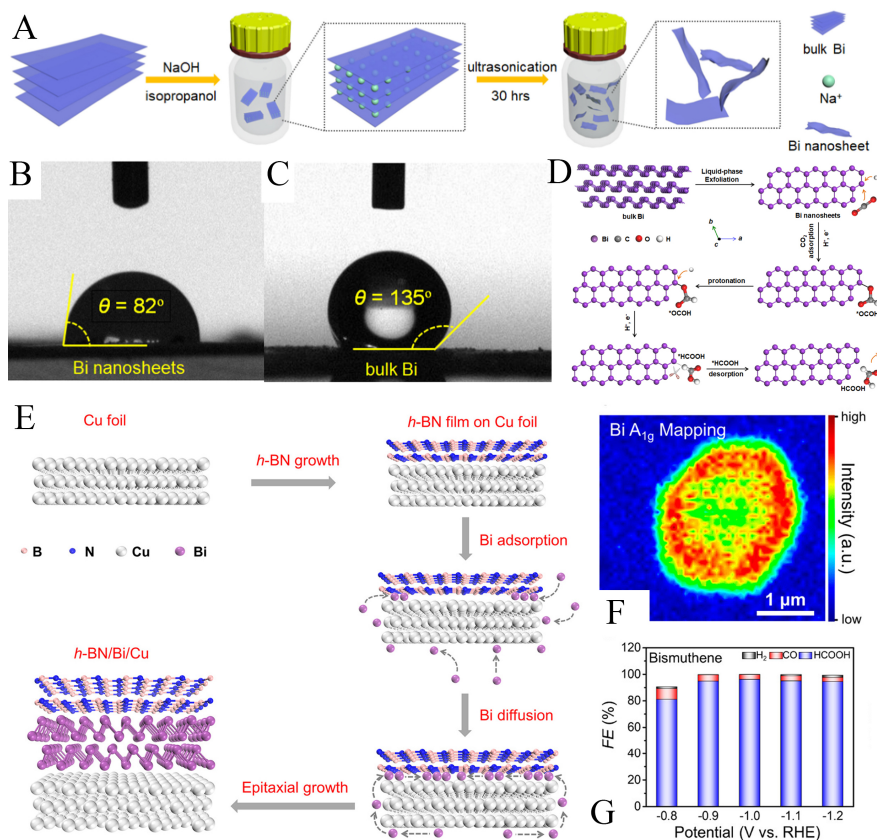
Figure 5. (A) Diagram of the preparation of Cu-doped Bi SACs; (B, C) Contact angle of Bi NSs and bulk Bi in aqueous solution; (D) Schematic diagram of the mechanism on Bi nanosheet. Reprinted with permission from Ref.[63]. Copyright 2018, Elsevier; (E) Schematic diagram of the growth mechanism of APCVD; (F) Corresponding Raman mapping of Bi A_{1g} peak intensity; (G) Electrochemical performance testing of bismuthene samples at different applied potentials (*vs.* RHE). Reprinted with permission from Ref.[64]. Copyright 2023, American Chemical Society. SAC: Single-atom catalysts; APCVD: atmospheric chemical vapor deposition.

configuration. Via subsequent electron and proton transfer, the intermediate to generate HCOOH is formed and consumed rapidly, thus greatly improving the FE of formate. Therefore, Bi nanosheets have high FE, moderate overpotential, and long-term stability for formate production in aqueous media, thanks to the excellent surface wettability of Bi nanosheets, which can be in full contact with the electrolyte [Figure 5B and C]. Bi nanosheets can also improve CO_2 absorption and provide better electron transport capabilities, enabling rapid formation and transfer of intermediates, and ultimately improve the selectivity of formic acid production [Figure 5D].

Hu *et al.* used hexagonal boron nitride (h-BN) layer encapsulation technology to epitaxial grow to-dimensional Bi nanosheets on copper foil by atmospheric chemical vapor deposition (APCVD)[64]. First, principle calculations and experiments show that an intermediate layer between h-BN and copper foil can be successfully fabricated using 2D Bi nanosheets. Detailed characterization confirmed that the fabricated Bi nanosheets have typical hexagonal single-crystal characteristics and do not contain any detectable impurities [Figure 5E and F]. The additional charge supply of the h-BN layer can effectively suppress the structural distortion of bismuth on copper foil, which is beneficial to the epitaxial growth of hexagonal Bi nanosheets by APCVD method to a large extent. The synthesized Bi nanosheets have single-crystal characteristics and large lateral size. In addition, under the protection of the h-BN top layer, the Bi nanosheet showed excellent thermal stability, which was not oxidized even after annealing at 500 °C at room

temperature, maintaining excellent stability. Finally, the electrocatalytic CO_2RR experiment confirmed that the Bi nanosheets involved in the CO_2RR process before the Cu region was not found had good performance in reducing CO_2 to formic acid, and had 96.3% ultra-high FE at -1.0 $V_{vs\,RHE}$ and -1.0 $V_{vs\,RHE}$ for a long time [Figure 5G]. During this process, Bi nanosheets are reconstructed and more active sites are generated. In Bi-based electrocatalyst, Bi nanosheets also maintains great long-term catalytic stability and excellent catalytic performance. DFT calculations show the charge transfer from the h-BN layer to the bismuth could compensate for the electron consumption and lead to a more stable structure. And the top h-BN layer is conducive to the formation and stability of 2D bismuth-ene. The sandwich epitaxial growth strategy provides favorable pathways for high surface energy materials in the range of h-BN encapsulation. In addition, the top layer can be replaced with another 2D material, thus expanding the fabrication range of 2D heterogeneous structures. As mentioned above, although 2D Bi-based nanomaterials series have effective CO_2RR catalytic activity, their catalytic performance still needs to be further improved. In particular, how 2D materials adjust the electronic structure and electron conduction path of the edge part and the middle part of the nanosheet is still worthy of further optimization to improve their catalytic performance of CO_2RR.

MODIFIED STRATEGIES AND BISMUTH OXIDE-BASED CATALYSTS

In the process of CO_2RR, the selectivity of the product is often affected by the side reaction HER. Several methods have been tried to inhibit HER and effectively reduce the activation energy of CO_2RR. The main purpose of improving CO_2 performance is to obtain high current density and FE with long-term stability over a low overpotential and wide potential range. The initial electron transfer to form the *CO_2 radical intermediate is essential for the activation and reduction of CO_2, which is widely regarded as the rate-determining step in the generation of HCOOH or CO. Therefore, it is fundamental to stabilize the catalytic active intermediates of CO_2. Metal oxide catalysts have inherent advantages in the adsorption of CO_2 intermediates by metastable oxygen. Unfortunately, metal oxide catalysts are self-reducing in the CO_2RR process because their reduction potentials are more accurate than those of CO_2RR. In the process of self-reduction of the reaction, its CO_2 electroreduction performance is seriously decreased. How to make its oxidation state stable and not reduced is an urgent problem to be solved.

Heterostructure strategy

By combining with multifunctional structures, heterogeneous structure engineering is an important approach to modulate reaction pathways in numerous catalytic processes. Coupling heterogeneous structure interfaces to achieve synergistic catalytic effects is crucial to regulating electron transfer, geometry, and interface coordination environment, thereby lowering the energy barrier of key reaction intermediates.

Feng *et al.* prepared a new sheet Bi_2O_3/strip BiO_2 heterojunction by top-down selective alkali-assisted dealuminization method using $Bi_2Al_4O_9$ [Figure 6A], and confirmed the existence of BiO_2 phase by X-ray diffraction spectroscopy (XRD), X-ray photoelectron spectroscopy (XPS), X-ray absorption near edge structure (XANES) and other test methods[65]. The Bi_2O_3/BiO_2 catalyst has the correct starting potential and high current density in the catalytic process, and the Tafel slope is also small, which indicates that the heterogeneous structure can reduce the reaction barrier of CO_2RR and benefit the response of CO_2RR [Figure 6B]. *In situ* tests showed that the Bi_2O_3 in the Bi_2O_3/BiO_2 heterojunction was completely reduced to metallic Bi under CO_2RR conditions [Figure 6C], and the catalysts have reconstructed from Bi_2O_3/BiO_2 to the new heterostructure Bi/BiO_2, thus continuing to act as an efficient catalytic active center. For the Bi/BiO_2 heterojunction, HER overpotential is 1.08 V, while the overpotential of CO_2RR to formate via the *OCHO pathway is only 0.19 V, and the overpotential of CO via the *COOH pathway is only 1.10 $V_{vs\,RHE}$ [Figure 6D]. That is, among the three competing cathodic processes, the reduction of CO_2 formation of
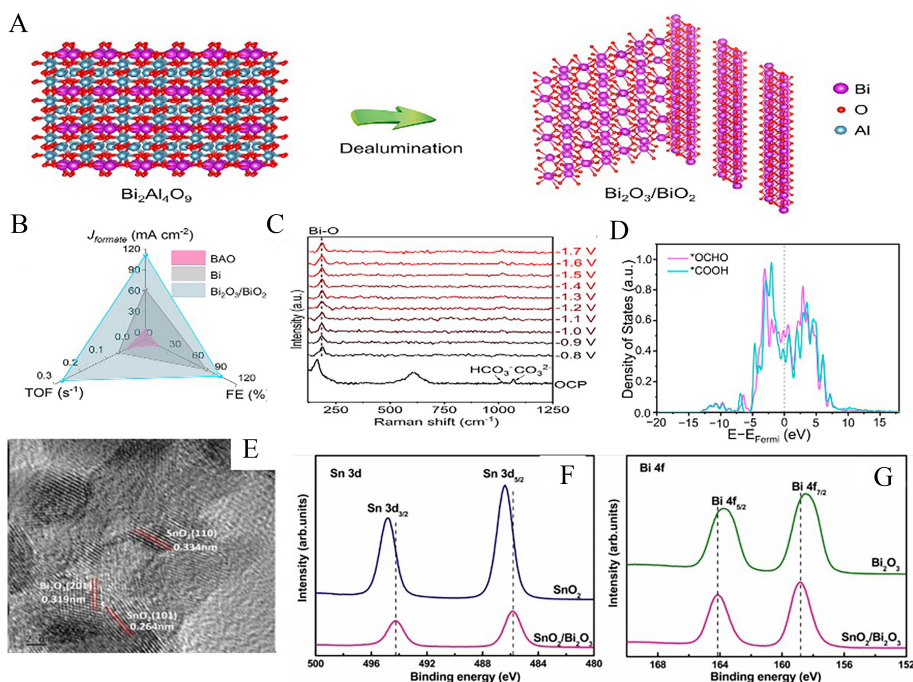
Figure 6. (A) Schematic synthesis of the Bi_2O_3/BiO_2 heterojunction; (B) XRD patterns of the Bi_2O_3/BiO_2 heterojunction. Comparison of TOF, electrochemical testing plots; (C) *In situ* Raman spectra of the Bi_2O_3/BiO_2 heterojunction during electrocatalysis; (D) DOS of the Bi p orbital with different intermediations adsorbed. Reprinted with permission from Ref.[65]. Copyright 2022, American Chemical Society; (E) HRTEM images of SnO_2/Bi_2O_3; (F, G) XPS spectra of SnO_2, Bi_2O_3, SnO_2/Bi_2O_3. Reprinted with permission from Ref.[66]. Copyright 2021, Wiley-VCH. XRD: X-ray diffraction spectroscopy.

formic acid is the most favorable in terms of energy and can effectively inhibit the HER process.

Tian *et al.* synthesized SnO_2/Bi_2O_3 heterostructures with SnO_2 clusters on Bi_2O_3 matrix[66]. Due to their different work functions, once they come into contact in the form of a heterojunction, a built-in potential is formed at the interface, equalization of their Fermi levels [Figure 6E]. During the catalytic reaction, interfacial electron transfer was observed between SnO_2 and Bi_2O_3, making SnO_2 at the electron-rich stage. The firm interfacial interaction protects the active site of SnO_2 from electrolytic reduction and achieves long-term electrochemical stability [Figure 6F and G]. This interfacial electronic effect significantly improves the CO_2 adsorption performance and the $*CO_2$ intermediate stability at high potentials. She is effectively inhibited at high potentials. DFT calculations show that the Bi_2O_3 support can improve the catalytic activity of CO_2 to HCOOH conversion. In particular, the synthesized SnO_2/Bi_2O_3 has a FE of 90% for C_1 products, including HCOOH and CO, at 1.0 V/RHE. FE of HCOOH has a wide potential range of from 1.0 to 1.4 $V_{vs\ RHE}$, and its potential remains above 76%.

Defects strategy

The importing of structural perturbations or defects can effectively affect the local electronic state and produce discordant sites with particularly high activity. Although the certain mechanism is dimness, defects strategy has been commonly used in various electrocatalysts[65,66]. The defective Bi oxide was designed as a template for cathodic conversion into defect-rich metallic Bi nanostructures for electrocatalysis of CO_2RR. Gong *et al.* developed a simple solution method to synthesize defective β-Bi_2O_3 double-walled NT[67]. Operational X-ray absorption spectroscopy (XAS) measurement displays that these oxide NT would be turned into defective Bi NT under cathode-polarization. When it was applied for CO_2RR, defective Bi NT

enables highly reactive and selective formic acid production. DFT studies have shown that this robust activity and selectivity can be on account of numerous defective Bi sites in the stable *OCHO intermediate.

Controlled morphology strategy

Gong *et al.* introduced poly (vinyl pyrrolidone) (PVP) as a structure guiding agent and prepared defective β-Bi_2O_3 double-wall NT by the controlled aqueous solution method[67]. The double-wall structure of the material and the surface coverage of highly defective fragments also provide a template for the cathodes to be converted into defective Bi metal nanostructures. Operational XAS measurements show that oxide NT can be converted into defective bismuth NT under cathode-polarization. DFT calculations also show that the presence of defects, whether 5-7 ring defects, single vacancies or double vacancies, facilitates the adsorption of stable *OCHO intermediates on the ideal Bi (001) surface, thereby facilitating the formation of formic acid. When applied for CO_2RR, it enables highly reactive and selective formic acid production.

Yang *et al.* studied the catalytic mechanism of Bi_2O_3[68]. They investigated the *in situ* structural reconstruction process from Bi@Bi_2O_3 nanodendrites (Bi@Bi_2O_3-NDs) to Bi nanoflowers (Bi-NFs) composed of ultra-thin 2D Bi nanosheets [Figure 7A]. Bi@Bi_2O_3-NDs grew on Cu foil. Besides, the activated Bi-NFs consisting of 3D self-assembled ultra-thin Bi nanosheets were finally formed by the two-step transformation of Bi@Bi_2O_3-NDs in $KHCO_3$ solution with bismuth oxycarbonate ($Bi_2O_2CO_3$, BOC) as an intermediate through *in situ* electroreduction. The extensive surface remodeling of Bi@Bi_2O_3NDs enables customized Bi-NFs electrocatalyst. Thus, Bi-NF has a FE of 92.3% at -0.9 $V_{vs\ RHE}$ and a high local current density of 28.5 mA·cm^{-2} at -1.05 V. In addition, the potential interface-dependent processes and mechanisms of Bi-NFs electrocatalysts in CO_2RR were investigated using *in situ* Raman spectroscopy. It is supposed that *OCHO is crucial in the formation of HCOOH, and that the surface remodeling and activation process of the active site of Bi-NFs is crucial to achieve the ultra-high selectivity of HCOOH [Figure 7B].

Tran-Phu *et al.* proposed an effective strategy to produce a fractal Bi_2O_3 catalyst layer for CO_2RR to formate by one-step magnification on a porous fiber substrate [Figure 7C][69]. This approach has several advantages, including the possibility to increase the electron density by tuning the physicochemical properties of Bi_2O_3. Furthermore, the fractal morphology of thermos-aerosol self-assembled Bi_2O_3 provides an open and homogeneous morphology, enabling efficient utilization of the deposited catalyst with a mass and current density three times higher than Bi_2O_3 collected when the filter cast CO_2RR nanoparticles on the same substrate. With richer electrons, Bi_2O_3 comprising metastable β phase Bi_2O_3 and abundant edge sites is highly selective for CO_2RR formation and exhibits 87% FE of HCOO$^-$ at -1.2 $V_{vs\ RHE}$, with an HCOO$^-$ current density of about -20.9 mA·cm^{-2} [Figure 7D].

Liu *et al.* successfully grew ultra-thin Bi_2O_3 nanosheets on conductive multi-channel carbon matrix (Bi$_2$O$_3$NSs@MCCM) by a simple hydrothermal method [Figure 7E][70]. This composite has several important advantages. Specifically, the nanostructured hollow mccm accelerated electron transfer, increased CO_2 adsorption, and increased the ratio of pyrrole-N to pyridine-N. Layered porous Bi_2O_3 nanosheets provide abundant active sites, reduce contact resistance and work function, and shorten the diffusion path of CO_2 saturated electrolyte. Importantly, Bi_2O_3NSs@MCCM can achieve relatively high current densities at moderate overpotential, allowing the conversion of CO_2RR to HCCOH to be selective, highly energy efficient, and with good long-term stability [Figure 7F]. As mentioned above, as a commonly used modification method, morphology control can not only play a crucial role in adjusting the catalytic site and catalytic activity, but also provide ideas for structural reconstruction. However, the choice of specific materials still needs to be made according to the material characteristics.
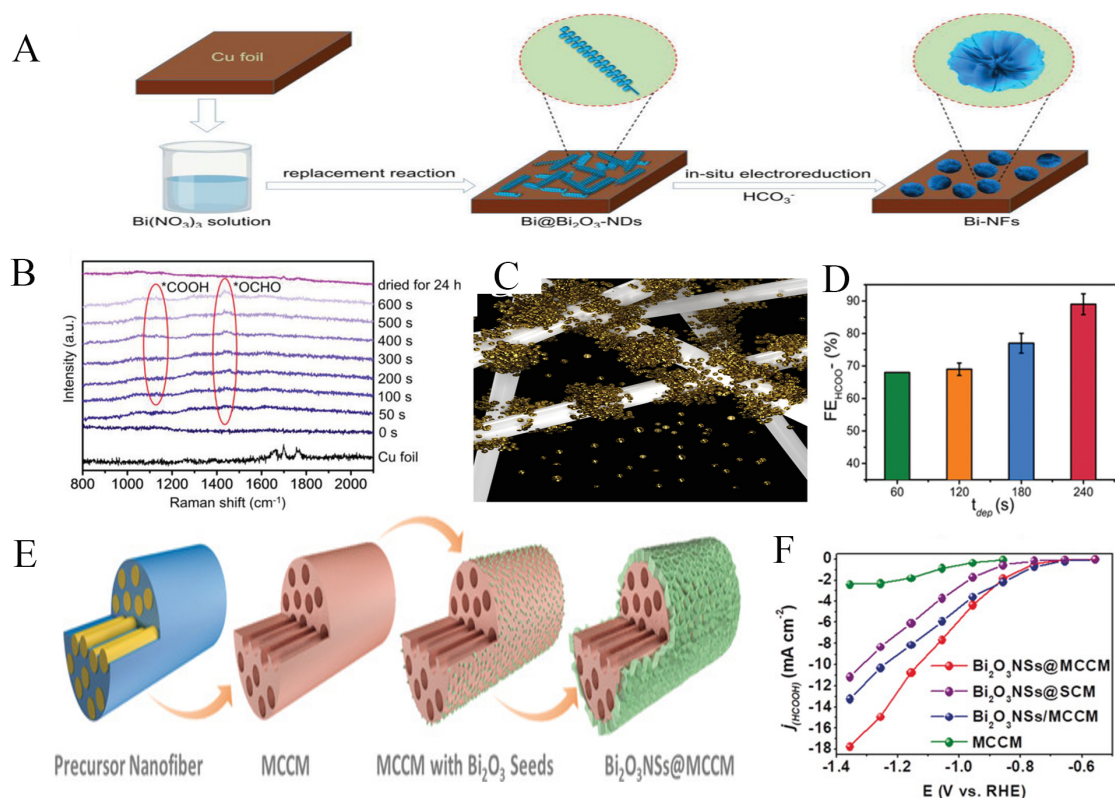
Figure 7. (A) Schematic illustration of the preparation process of Bi-NFs *in situ* synthesis on Cu foil; (B) *In situ* Raman spectra characterization derived from Bi-NFs. Reprinted with permission from Ref.[68].Copyright 2023, Wiley-VCH; (C) SEM characterization of the Bi_2O_3; (D) FE formate plots as a function of different deposition times. Reprinted with permission from Ref.[69].Copyright 2019, Wiley-VCH; (E) Illustration of the formation process of the Bi_2O_3NSs@MCCM; (F) $j_{(HCOOH)}$ of the Bi_2O_3NSs@MCCM and other comparison samples. Reprinted with permission from Ref.[70].Copyright 2019, Wiley-VCH. FE: Faraday efficiency; Bi-NFs: Bi nanoflowers.

Bi-based core-shell electrocatalysts

On account of relatively low conductivity and selectivity, Bi-based oxides tend to exhibit poor activity at low and wide cathodic potential Windows. A feasible strategy to improve conductivity is to synthesize core-shell structured nanocatalysts with highly conductive metal cores and lamina metal oxide shells, which may optimize electronic properties and intermediate bond strengths[71,72]. To further improve the activity of electrocatalysts, the design of novel Bi-based materials in combination with other components has become an effective strategy to regulate the adsorption, activation and desorption of reactants. Zhao *et al.* prepared a novel Sn-doped Bi/BiO_x NW with a highly conductive bimetallic core and an amorphous Sn-doped BiO_x shell by electrochemical dealloying [Figure 8A][73]. Sn atoms in the Bi_2O_3 and BiOx lattices are supposed to cooperate with oxygen atoms in an octahedral form. $Bi/Bi(Sn)O_x$ NWs have a metallic binuclear structure [Figure 8B-D]. Compared with reversible hydrogen electrodes, these NWs showed excellent CO_2RR activity in a wide potential window, selectively generated formate, and achieved FE in the range of -0.5 to -0.9 V (*vs.* RHE). The maximum FE at -0.7 $V_{vs\,RHE}$ gas diffusion cell is 98 ± 2% [Figure 8E]. DFT calculations reveal that the $Bi/Bi(Sn)O_x$ catalyst showed a lower energy barrier (ΔG) for *OCHO formation, suggesting that the Sn-doped BiO_x shell can greatly promote *OCHO formation. The incorporation of Sn atoms into BiO_x modulates the electronic properties of Bi and allows the adsorption of *OCHO intermediates on the $Bi(Sn)O_x$ surface, while increasing formic acid production by inhibiting the competing HER [Figure 8F]. In summary, Table 2 compares the best FE of bismuth oxide-based catalysts. It can be seen that the listed materials have good FE of bismuth oxide compounds and formic acid through different modification

Table 2. FE of bismuth oxide-based catalysts

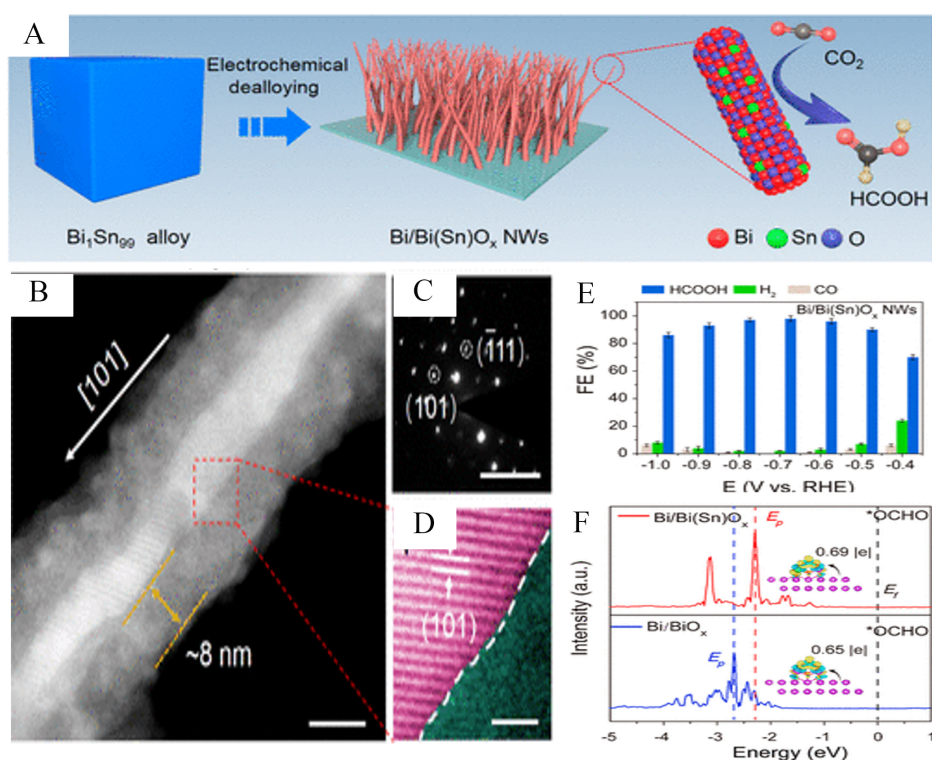| Materials	FE/%	Ref.
Bismuthene	98.12	[64]
SnO_2/Bi_2O_3	~80	[66]
$\beta\text{-}Bi_2O_3$	87	[67]
$Bi@Bi_2O_3\text{-}NDs$	92.3	[68]
$Bi_2O_3NSs@MCCM$	93.8	[70]
$Bi/Bi(Sn)O_x$ NWs	~100	[73]

Figure 8. (A) Schematic diagram of the synthesis of Sn-doped Bi/BiO_x nanowires; (B-D) HAADF-STEM characterization diagrams; (E) Different products FEs of the $Bi/Bi(Sn)O_x$ NWs; (F) P-orbital DOS plots of absorbed with *OCHO on Sn-decorated Bi/BiO_x nanowires and Bi/BiO_x nanowires. Reprinted with permission from Ref.[73]. Copyright 2021, American Chemical Society. FE: Faraday efficiency.

strategies, so the above modification strategies have good effects on bismuth oxide.

OTHER BISMUTH COMPOUND-BASED CATALYSTS

Bismuth subcarbonate-based catalysts

Among Bi-based compounds, BOC is considered a valuable electrocatalyst for CO_2RR to formate on account of its significant advantages: (1) A large number of Bi-O bonds in BOC can promote the adsorption of CO_2 and production and transformation of intermediates during the CO_2RR process; (2) BOC species of carbonate enable to enhance the adsorption of initial intermediates[74-76]. Therefore, it is attractive to ulteriorly develop electrocatalysts based on the advantages of BOC for efficient generation of CO_2RR within a wider potential window.

Fu *et al.* reported a method for electrochemical conversion of bismuth oxychloride (BiOCl) to basic bismuth carbonate containing chlorine [$Bi_2O_2(CO_3)_xCl_y$] under the condition of CO_2RR[77]. It is proved that *in situ* synthesis is an effective method to improve the electrochemical stability of electrocatalyst *in situ*. *In situ* spectroscopic studies were systematically performed to describe the conversion mechanism and electrochemical stability. BiOCl is converted to BOC by anion exchange [Figure 9A]. The fabricated $Bi_2O_2(CO_3)_xCl_y$ tolerates -1.0 V (relative to RHE), while the wet chemically synthesized pure BOC undergoes metal Bi^0 formation at -0.6 $V_{vs RHE}$, implying a significant increase in electrochemical stability. No significant structural changes and performance degradation were observed when $Bi_2O_2(CO_3)_xCl_y$ was stabilized at a voltage of -0.8 V relative to RHE for 20 h [Figure 9B]. At a voltage of -0.8 $V_{vs RHE}$, $Bi_2O_2(CO_3)_xCl_y$ can easily achieve 97.9% FEHCOO⁻, which is much higher than BOC (81.3%). DFT calculations show that, unlike the generation of HCOOH from CO_2RR catalyzed by BOC, the generation of HCOOH on $Bi_2O_2(CO_3)_xCl_y$ through the *COOH intermediate step requires an energy input of 2.56 eV.

Wu *et al.* prepared In-doped BOC nanosheets (BOC-In-X NSs) via electrochemical operando deposition and electrochemical reduction [Figure 9C][78]. At a voltage of 0.9 V, the FE of formate of BOC-In-0.1NS is the highest with 98.3%, and it has good stability for 22 h. In addition, FE formate achieves an average of 93.5%. DFT calculations show that compared with BOC (-1.801 eV), the E_d of BoC-In (-1.780 eV) is closer to the Fermi level (E_f), and the E_p of BOC-In (-1.492 eV) moves more closely to the E_f, which illustrates that BOC-In is more conducive to the occurrence of catalytic reactions [Figure 9D and E]. The energy barrier on the BOC NS (010) surface (0.55 eV) is much higher than that of In-doped BOC NS (0.48 eV) [Figure 9F]. And the addition of BOC not only enhances the adsorption of CO_2, *CO_2- and *OCOH intermediates, but also reduces the energy barrier of *OCOH to form formic acid, which is conducive to the formation of formic acid.

Bi sulfide-based catalysts

Sulfur atom doping can activate bismuth-specific sites while passivating edge sites, thus promoting the production of highly selective and reactive formic acids, providing high catalytic activity to CO_2RR. From a thermodynamic point of view, sulfur atoms prefer edge sites of metal catalysts, and the addition of sulfur changes the electronic structure of adjacent sites, hence increasing the catalytic activity of metals. In addition, the binding of S to the metal edge site occupies the adsorption site of *H, thus inhibiting the main competitive reaction of HER. Therefore, the addition of S enables selective improvement of the performance of CO_2RR.

Lv *et al.* designed Bi nanosheets with numerous edge defect sites coordinated with sulfur atoms by electrochemical reconstruction of $Bi_{19}Br_3S_{27}$ NW (BBS) [Figure 10A][79]. The marginal sulfur bismuth catalyst increased the yield of formate and inhibited the precipitation of hydrogen. During the structural transition, the BBS precatalyst is reconstructed into the metal Bi with abundant defects, and the Br atom escapes completely as HBr. *In situ* EXAFS characterization shows that Bi atoms are reconstructed during the catalytic process, which has a significant effect on catalysis [Figure 10B]. DFT and characterizations display sulfur atoms tend to appear in the margin region of the defect, reducing the density of coordinated unsaturated Bi sites for *H adsorption, while adjusting the adjacent Bi sites in the center of the p-band to obtain better CO_2RR performance [Figure 10C]. Under alkaline conditions, formic acid exhibits high FE (~95%) [Figure 10D].

Wang *et al.* developed an atom-dispersed N and S-coordinated bismuth-atom site catalyst (Bi-SAs-NS/C) for electrocatalytic CO_2 reduction through simultaneous cation and anion diffusion strategies[80]. Bi is then trapped by abundant nitrogen-rich vacancies, and S binds to the carbon support at high temperatures to
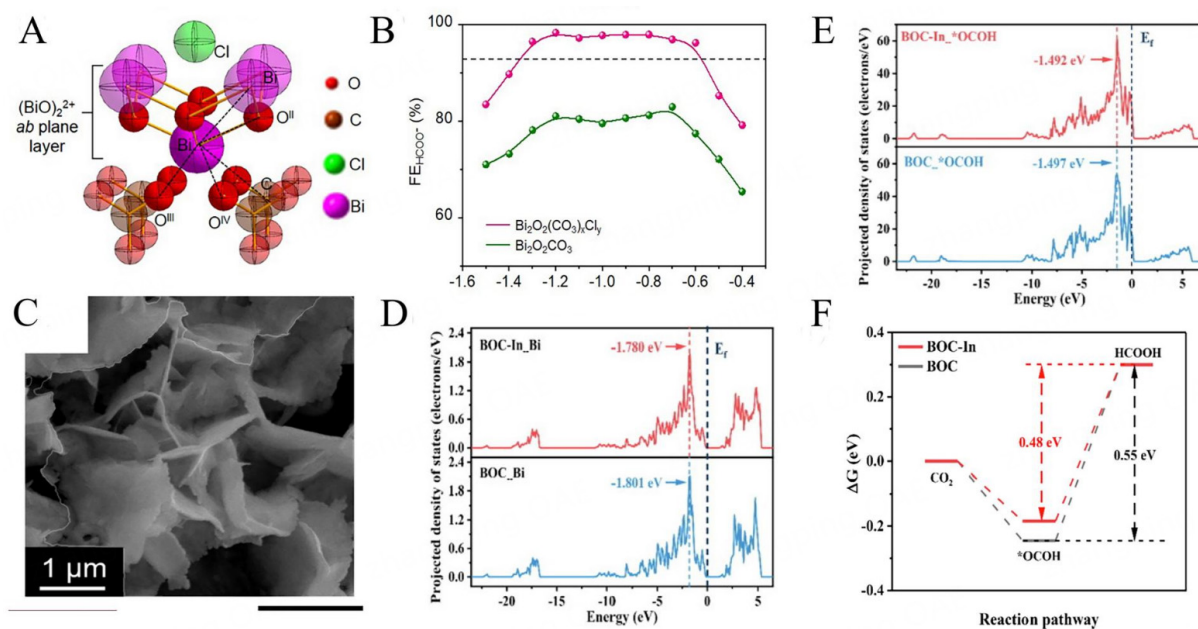
Figure 9. (A) 3D configuration of bismuth carbonate containing chlorine; (B) Plots of Faradic efficiency for CO_2RR at different potentials (*vs.* RHE). Reprinted with permission from Ref.[77]. Copyright 2022, Springer; (C) Surface characterization of the BOC-In-0.1 NSs; (D) Projected density of states (PDOS) of d-band centers of Bi atoms, (E) the Bi site absorbed with *OCOH and (F) calculated free energy diagrams for the electroreduction of CO_2 to HCOOH on the (001) facets of BOC and BOC-In. from Ref.[78]. Copyright 2022, Elsevier.

form the Bi coordination of N and S. On account of the simultaneous diffusion of Bi atoms and sulfur, nitrogen atoms with different electronegativity, the catalysts can effectively cooperate with Bi to form homogeneous Bi-N$_3$S /C sites. The prepared Bi-SAs-NS/C showed high selectivity for /CO, with a FE of over 88% over a broad potential range and a maximum of 98.3% FE of CO at a current density of 10.24 mA·cm^{-2} at -0.8 V$_{vs\ RHE}$. Within 24 h, the continuous electrolysis can be kept constant with negligible degradation. DFT calculations show that the catalytic performance of Bi-SAs-NS/C is significantly better than that of Bi-SAs-N/C, due to the substitution of the ligand N in the center of Bi-N$_4$C by the less electroactive S, which greatly reduces the energy barrier formed by the intermediate in the rate-limiting step and improves the reaction kinetics.

Bi halide-based catalysts

A number of recent studies have revealed possible effects of halides on CO_2RR activity. Surface modification of halides can be directly introduced into electrolyte or cathodic conversion of metal halides. They can affect the charge distribution on the surface of the metal catalyst and thus regulate the relative binding strength of key intermediates.

Luo *et al.* designed bismuth halide perovskite as a precatalyst according to the characteristics of halide anions and alkali metal cations, and used the metal-air battery cathode to prepare bismuth co-modified by halide and alkali metal as a working catalyst[81]. They used a modified heat injection method to prepare hexagonal Cs$_3$Bi$_2$I$_9$ nanocrystals and introduced long-chain ammonium oil palm amI-I (OAMI-I) to slow down the nucleation and growth of perovskite nanocrystals [Figure 11A]. The results show that the modified Cs$_3$Bi$_2$I$_9$ catalyst provides an industrial-scale current density of 300 mA·cm^{-2} and an 87% FE for formic acid in the flow cell [Figure 11B]. Moreover, after assembly in Al-CO$_2$ cells, Cs$_3$ Bi$_2$ I$_9$ exhibits a very high current density (69 mA·cm^{-2}) with a peak power density of about 7 mW·cm^{-2}.
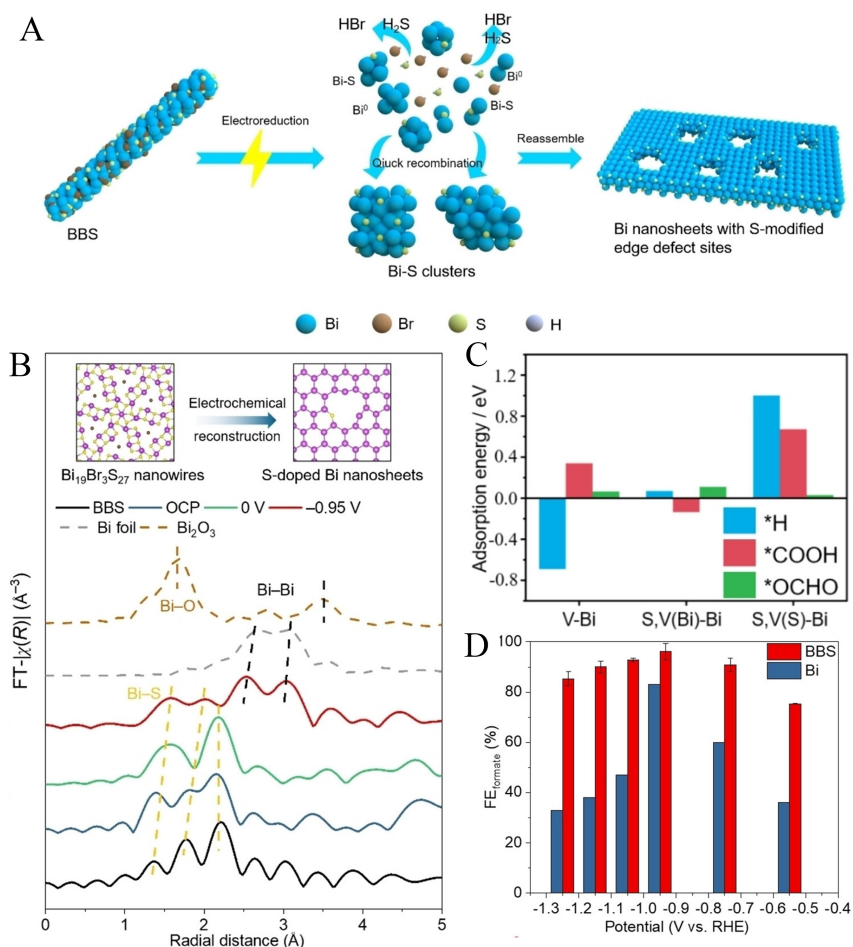
Figure 10. (A) Schematic illustration of the transition from BBS to Bi nanosheet; (B) *In situ* FT $k_3\chi(R)$ EXAFS of Bi L_3-edge EXAFS signals; (C) Calculated adsorption energy plot for the electroreduction of CO_2 to HCOOH through different intermediations on sample catalysts; (D) FE of formate of BBS sample and Bi sample. Reprinted with permission from Ref.[79]. Copyright 2023, Wiley-VCH. EXAFS: Extended X-ray adsorption fine structure; FE: faraday efficiency; BBS: $Bi_{19}Br_3S_{27}$ NW.

Yang *et al.* synthesized layered oriented double halide oxide (BiOX, where X = Cl, Br or I) nanosheets [Figure 11C][82]. Operando XRD and Operando Raman spectroscopy measurements were performed to track the kinetics of the *in situ* conversion of the BiOX catalyst material to the active metallic Bi electrocatalyst [Figure 11D]. It was supposed that *in situ* activated dielectric catalysts expose specific crystal planes, depending on the choice of halide: Br$^-$ promotes Bi (003) exposure, Cl$^-$ leads to dominant Bi (012) crystal planes, and I$^-$ produces mixtures. In addition, we relate surface exposure to catalytic properties. Compared with reversible hydrogen electrodes, BiOBr (BOB) showed HCOOH selectivity of up to 91% at a current density of 148 mA·cm^{-2} at -1.05 $V_{vs\ RHE}$. BiOCl exhibits a HCOOH FE of 69% at a current density of 88 mA·cm^{-2} and a potential of -1.09 V. BiOI (BOI) showed 76% selectivity for HCOOH at 95 mA·cm^{-2} current density, while RHE was between BOB and BiOCl at -1.08 V current density. This suggests that the Bi (003) base surface formed *in situ* is more catalytic than the stepped Bi (012) site. Furthermore, *in situ* XAS measurements indicate that BiOCl restructures rapidly after the onset of reduction and exhibits transient transition states, while the transition states of BOB and BOI are longer lasting.

Wang *et al.* used bismuth halide ($Bi_4O_5Cl_2$, $Bi_4O_5Br_2$ and BiOI) as a precatalyst to study the effect of halogen on the *in situ* conversion of BiOI in CO_2RR [Figure 11E][83]. Among them, BiOI *in situ* transformed Bi NSs
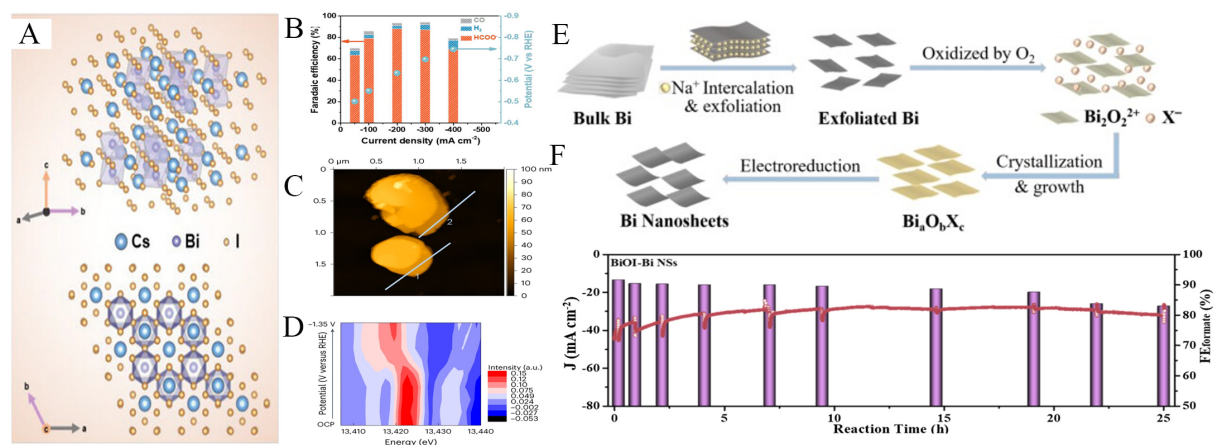
Figure 11. (A) Structural model diagram of $Cs_3Bi_2I_9$; (B) Electrochemical properties of different products. Reprinted with permission from Ref.[81]. Copyright 2023, Wiley-VCH; (C) AFM image of BiOX sample; (D) In-BOB, measured at -1.15 $V_{vs\,RHE}$ and plotted as normalized intensity versus energy. Reprinted with permission from Ref.[82]. Copyright 2023, Springer; (E) Schematic diagram of the preparation of bismuth halide and reaction process to Bi NSs; (F) Electrochemical property testing of sample. Reprinted with permission from Ref.[83]. Copyright 2022, Elsevier. BOB: BiOBr.

showed high CO_2RR selectivity. The FE of formate (*vs.* RHE) is greater than 90% in the range of -0.71 to -1.0 V (all potentials of RHE are as follows). FE formate was highest at -1.0 V, which was 91.33% ± 0.58%. The *in situ* FE formate of both $Bi_4O_5Br_2$ and $Bi_4O_5Cl_2$ was below 86% at the selected application potential [Figure 11F]. The *in situ* transformed bismuth oxide halide was analyzed by XPS and only type I residue was detected. In summary, Table 3 compares the optimal FE of other types of Bi-based materials, and it can be seen that by passing carbonate, bismuth sulfur-based catalyst pairs well with bismuth halide compounds, especially for formate formation.

APPLICATION OF IN SITU TECHNIQUE IN INVESTIGATING THE BI-BASED CATALYSTS FOR CO₂RR

Catalytic reaction pathways and intermediates play a crucial role in the catalytic process. At present, although many studies have greatly improved the catalytic efficiency, there are still many problems in the monitoring of catalytic intermediate processes. In particular, the CO_2RR reaction process involves multiple electron transfer and proton transfer. The study of its process helps us not only optimize the reaction path and design the catalyst, but also understand the reaction process more deeply from the perspective of electrons. However, *in situ* characterization technology can effectively monitor the reaction structure and reaction intermediates of the catalyst, and has a unique role in revealing the catalytic mechanism. A variety of advanced characterization techniques, including Raman spectroscopy, infrared spectroscopy (FTIR), XAS, XRD and XPS, have been used for real-time CO_2RR studies. Next, we discuss how *in situ* techniques can be effectively used to reveal the reaction process.

In situ/operando raman spectroscopy

Raman spectroscopy can determine the vibrational modes of molecules and identify intermediate species. Molecules with different vibrational/rotational states can be detected by measuring the energy difference between the incident and inelastically scattered photons. Raman spectroscopy has a great advantage in identifying metastable catalysts and intermediates[37].

Li *et al.* used *in situ* Raman to demonstrate that the prepared 2D Bi_2O_3 nanosheets were used as precursor templates to directly synthesize well-defined Bi nanoribbons[84]. The activated Bi-O sites in high temperature

Table 3. FE of Other bismuth compound-based catalysts

Materials	FE/%	Ref.
$Bi_2O_2(CO_3)_xCl_y$	97.9	[77]
BBS	95	[79]
Bi-SAs-NS/C	98%	[80]
rCBI	98.2%	[81]
BOI	96%	[82]
BiOI-Bi NSs	91.33 ± 0.58	[83]

treatment remained stable throughout the CO_2RR process. As a result, the resulting one-dimensional Bi heterostructures exhibit excellent CO_2RR properties with high formic FE over a wide and mild potential range (approximately 95%), as well as the impressive stability of 100 h of continuous operation under a variety of conditions without attenuation [Figure 12A]. Zhao *et al*. used the transfer of Raman peaks *in situ* Raman tests at different potentials to show that the Bi-O structure in BOC after reaction is more likely to be restored[85]. Combined with the above *in situ* study under CO_2RR, we obtained a detailed hypothesis of the evolution of BOS to BOC after reaction structure; that is, BOS was first completely transformed into BOC, and then part of BOC was cathodically reduced to metallic Bi under CO_2RR conditions. To demonstrate the stability of the Bi-O substance in surface-oxygen-rich carbon-nanorod-supported bismuth nanoparticles (SOR Bi@C NP), Liu *et al*. performed *in situ* Raman spectroscopy to understand how the catalyst surface structure changes with the applied reduction potential[86]. They observed the appearance and disappearance of Bi-O characteristic bands at different potentials, demonstrating the stability of the Bi-O substance. These ectopic and *in situ* characterization techniques indicate that oxygen-enriched SOR Bi@C NP is structurally stable during CO_2RR. The formation of *OCHO intermediates on Bi-O/Bi (110) is considered to be the rate-determining step, and the Bi-O/Bi (110) structure is the root of the excellent CO_2RR performance in SOR Bi@C NP. Liu *et al*. explored the surface transition mechanism of BOC@Bi/CP (carbon paper) electrodes by *in situ* Raman spectroscopy[87]. The reduction of BOC on the surface to Bi by Raman spectroscopy proves that flower-like Bi nanosheets can provide sufficient reaction sites to regenerate bismuth oxide (BO) on the surface in a CO_2-rich environment during continuous reduction. Moreover, even under the relative negative potential (~0.90 V *vs*. RHE) during the polyphase electrocatalysis, the composite does not reduce[88].

In situ/operando infrared spectrum
In situ FTIRs is a combination of electrochemical measurement methods and infrared spectroscopy technology, real-time monitoring of the catalytic reaction occurring at the gas-liquid-solid three-phase interface, at the molecular level to obtain reactants, target products, electrode surface bonding, intermediates and other information.

Cao *et al*. pioneered an atomically thin bismuthene (Bi-ene) through an *in situ* electrochemical transformation process of an ultra-thin bismuth group organic layer[50]. *In situ* attenuated total reflection infrared (ATR-IR) and DFT results confirmed that the adsorbed HCO_3^- groups in the electrolyte played an important role in the CO_2RR process. *In situ* infrared spectroscopy can also be used to further analyze the catalytic local reaction microenvironment and the adsorption capacity of CO_2 in the three-phase interface, so as to further understand the gas adsorption process of the reaction. According to the spectral band analysis [Figure 12B], BOC NF (bismuth subcarbonate nanoflowers) and Bi have high physical adsorption capacity, but Bi has almost no chemical adsorption capacity. Compared with Bi_2O3, BOC NF also has a high adsorption capacity for carbon dioxide[89].
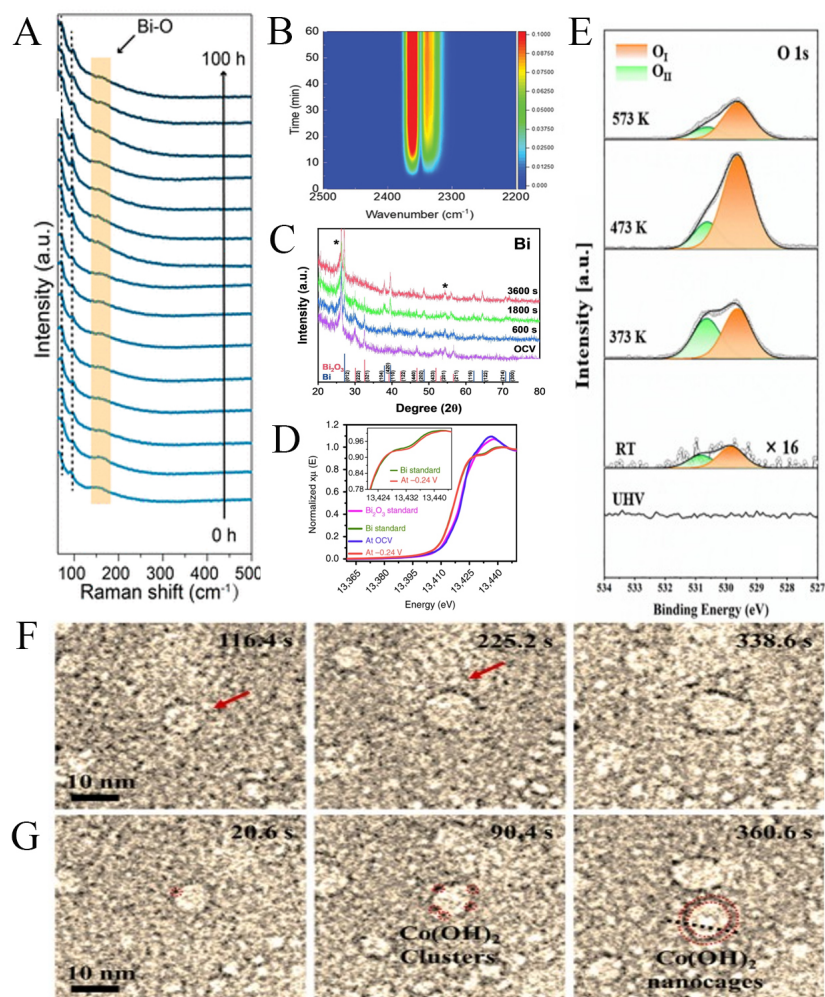
Figure 12. (A) *In situ* Raman spectra of two-dimensional Bi nanosheets. Reprinted with permission from Ref.[84].Copyright 2022, American Chemical Society; (B) *In situ* DRIFTS spectra of CO_2 adsorbed on BOC NFs surface. Reprinted with permission from Ref.[89]. Copyright 2022, Wiley-VCH; (C) *In situ* XRD patterns of Bi catalysts. Reprinted with permission from Ref.[91].Copyright 2021, Elsevier; (D) Operando Bi L-edge XANES spectra of Bi_2O_3 nanotubes (NTs) at OCV and NTD-Bi; inset plot is the partially enlarged spectra. Reprinted with permission from Ref.[67].Copyright 2019, Springer; (E) *In situ* XPS measurements for O 1 s orbit. Reprinted with permission from Ref.[92].Copyright 2022, Elsevier; (F, G) Formation of Co-TMH clusters and nanocage around the nanobubble surface. Reprinted with permission from Ref.[94].Copyright 2022, Elsevier. XRD: X-ray diffraction spectroscopy; XANES: X-ray absorption near edge structure; OCV: open circuit voltage.

In order to better understand the role of Te and Bi species in CO_2RR, Cui *et al*. used *in situ* attenuated total reflection surface-enhanced infrared absorption spectroscopy (ATR-SEIRAS) to monitor adsorbed species on the electrochemical surface[90]. The experiments show that the consumption rate of the reaction intermediate increases, which leads to a faster conversion to HCOOH, indicating that the Te-doped Bi catalyst can effectively accelerate the reaction. The peak intensity indicated that the intermediate accumulates at the interface, which may be related to the slower kinetics of the HCOOH reaction.

Other in situ/operando characterizations

Many other *in situ* testing techniques are gradually being applied to CO_2RR. Li *et al*. used *in situ* XRD analysis to reveal the structural evolution of Bi catalyst during CO_2RR processes [Figure 12C][91]. For the Bi catalyst under open circuit voltage (OCV) condition, the phase transition from Bi_2O_3 to metallic Bi was proved by the change in the position of the derived peak during the process, and the phase transition was

completed within one hour after the reduction potential was applied. Gong *et al.* performed *in situ* XAS measurements at the Bi L edge[67]. The Bi edges of XANES under OCV conditions are well aligned with Bi_2O_3 reference Bi edges [Figure 12D]. When the electric potential is reduced to -0.24 V, the feature of the Bi (III) edge at 13.423 keV gradually changes to a lower energy of 13.417 keV, which is aligned with the XANES edge of Bi metal foil. Zhang *et al.* used *in situ* XPS analysis of Bi4f spectra to reveal that the degree of Bi oxidation of BiCu with varying Bi layer thicknesses differed during exposure to CO_2 [Figure 12E][92]. This indicates coverage dependence of Bi oxidation at the Bi-Cu interface with exposure to CO_2. Since oxidation of Bi is caused by activation and dissociation of CO_2 on BiCu (111), dissociation of CO_2 and oxidation of Bi correspondingly become difficult or energy intensive as Bi coverage on Cu (111) increases, which, in turn, requires further enhanced annealing. Using quasi *in situ* XPS analysis, Jiang *et al.* showed that nanoclusters maintain their oxidation state (+3) during CO_2RR and BiO clusters are much more resistant to reduction under CO_2RR compared to bulk Bi oxide, where all Bi atoms are present on the surface and in low-coordinated clusters[93]. In the surface studies, *in situ* electron microscopy is often used to monitor transient structures and measure the reaction kinetics of nanostructure transformation. *In-situ* transmission electron microscopy (TEM) can provide vital information about the reactions on modified surfaces as well as the catalytic reactions and the growth of thin films or nanocrystals. Experiments involve exposing the sample to the reaction environment while imaging under conditions sensitive to changes in the sample surface rather than inside the sample. The reaction environment can include high temperature, reaction gas flow, deposition flow, or even exposure to a liquid environment. Therefore, *in situ* TEM also has applications in the field of CO_2RR. Through *in situ* TEM analysis and diffusion theory derivation, Xiao *et al.* found that the diffusion rate of the reaction system is positively correlated with the temperature, and negatively correlated with the system viscosity, and the system viscosity is negatively correlated with the temperature[94]. Porous MOF derivatives were synthesized *ex situ* at -80 °C [Figure 12F and G]. However, at room temperature, when the diffusion coefficient of the system is large, hollow MOF derivatives composed of nanosheets are formed. However, the porous derivatives have more surface unsaturated sites and reactive active sites. In order to understand the important role of the structure of the molecular catalyst in the CO_2 reduction process at the gas-liquid interface of the microdroplet. A series of mass peaks associated with Cu (1)-containing catalysts were observed by *in situ* mass spectrometry[95]. The high abundance of the monovalent Cu species confirms its potential role as an electron reservoir/transfer agent within the microdroplet, which facilitates the subsequent chemical transformation.

CONCLUSIONS

Recently, many studies have been conducted to improve the performance of CO_2RR, especially in the non-toxic catalyst[96,97]. These research strategies mainly focus on atom doping, heterogeneous structure formation, defect engineering, core-shell structure development, and so on. However, for Bi-based materials, there remains significant room for improvement in the performance of CO_2RR, and there is also great demand for improvement in the subsequent commercialization. In order to further enhance the activity and stability of the catalyst and better design the subsequent catalyst from the mechanism, we propose the following aspects.

In order to improve the selectivity and activity of the catalyst, increasing the catalytic site is an important research idea, and many modification strategies are also studied based on this. Nanoengineering can greatly reduce the size of the catalyst, increase the specific surface area of the catalyst, and expose more catalytic sites, so as to achieve the purpose of improving performance. From the perspective of catalyst scale, the mono-atomic catalyst can effectively realize the dispersion of the catalyst and maximize the surface area. One-dimensional materials have unique advantages for the addition of catalytic sites and electron transport due to their large aspect ratio. Many Bi-based materials have a graphene-like 2D structure, which also has

significant advantages in electron transport and catalytic activity[97]. In addition, in electrochemical catalysis, the electron transfer and the optimization of electronic structure are also the points that need constant attention. Atomic doping and alloy can regulate the electron distribution of Bi-based catalyst by introducing other elements, and the core-shell structure can also optimize the catalytic process by electron transport between the core and shell.

In order to further understand the catalytic reaction process, the use of *in situ* testing techniques becomes important. Previous tests often only monitor the initial and final states of the reaction, so the changes of the reaction intermediates in the catalytic process and their interaction with the catalyst are not very accurately understood. However, *in situ* technology can effectively solve this problem, so as to further understand the catalytic process, thereby further designing the catalyst and reaction conditions. *In situ* spectroscopic characterization can provide in-depth details about structural and surface properties during catalyst reactions, including phase transitions, electron transfer paths, catalyst binding configurations, and intermediate binding structures. Therefore, the selection of appropriate real-time detection is of great significance for the design of high purity catalysts. At present, although many *in situ* technologies have been very mature, how to effectively combine them with the catalytic process for monitoring is worth further exploration. In addition, the use of *in situ* electron microscopy and *in situ* light microscopy is still insufficient, and the change of surface morphology is worth further study. In addition, polarization orientation can regulate the reactivity and selectivity of various catalytic reactions by adjusting various basic properties (such as electronic and adsorption properties)[98]. *In situ* technology can be used to monitor the mechanism of polarization in CO_2RR, which can effectively reveal the effect of polarization on catalysts.

In addition to *in situ* monitoring techniques, DFT calculations can be used to predict thermodynamic and kinetic changes in the process through theoretical simulations, so as to design specific catalyst structures. However, with the development of computing technology, how to effectively combine DFT calculation results with actual experiments is still worth further exploration. In addition, accurately simulating the real situation of the catalyst surface, including the simulation of the reaction environment such as electrolyte and electric field, continues to pose challenges. In addition, the introduction of artificial intelligence (AI) into catalyst design can optimize the design simulation and calculation of batch catalysts, so as to greatly improve the efficiency of catalyst design.

In addition to material design and characterization technology, CO_2 electrocatalytic reaction design should also be oriented to industrial practical applications. Compared with H and flow cells, MEA cells have advantages in the transport of reactants, such as the diffusion of carbon dioxide solubility in aqueous solution, and can effectively improve the reaction stability.

Moreover, most of the CO_2RR in the current study occurred in alkaline electrolyte environments[99-102]. However, the locally strong alkaline environment leads to carbonate formation, resulting in limited single-pass carbon efficiency[103]. In addition, carbonate crossover to the anode and subsequent CO_2 release can further raise the cost of CO_2 separation from the O_2 stream at the anode. Switching to an acidic environment offers a fundamentally different approach to addressing CO_2 utilization constraints[104]. In acidic environment, when hydrogen hydrate (H_3O^+) is used as the proton source of CO_2RR, OH- will not be formed. Therefore, carbonates are generated without carbon dioxide consumption, which in principle minimizes carbonate formation and thus alleviates CO_2 penetration[105]. At present, Li *et al.* have tried to apply Bi-based catalysts to acidic CO_2RR, and used vertically grown Bi-based nanosheets to construct a cavity as an ideal electrolyte reservoir, creating an electrolyte-reservoir concept in a local high alkalinity region, and still achieving more than 80% FE under acidic conditions[106]. Therefore, there will be further

development of Bi-based catalyst in inhibiting HER of CO_2RR in acidic or neutral environment, improving FE and device-making in the future.

In summary, this paper introduces and discusses the application of Bi-based electrochemical catalysts in CO_2RR. At the same time, further development should rely on the combination of advanced *in situ* characterization techniques, in-depth understanding of the reaction mechanism, optimization of the electrocatalyst, and improvement of the battery configuration. It is believed that with continuous efforts, carbon recycling and zero emissions will be driven by sustainable energy to achieve further advancement of CO_2RR.

DECLARATIONS

Authors' contributions
Drafted the manuscript: Zhang, C.; Liu, F.
Participated the writing and literature discussion: Zhang, C.; Liu, F.; Wang, J. J.; Wang, G. J.; Sun, Z. Y.; Chen, Q.; Han, X. P.; Deng, Y. D.; Hu, W. B.
Coordinated the writing and finalized the manuscript: Wang, JJ.; Wang, G. J.

Availability of data and materials
The data that support the findings of this study are available from the corresponding author upon reasonable request.

Conflicts of interest
All authors declare that they are bound by confidentiality agreements that prevent them from disclosing their conflicts of interest in this work. Yi-Da Deng is an Editorial Board Member of the *Microstructures.* Zhao-Yong Sun and Qiang Chen were employed by China Energy Lithium Co. All other authors have no conflict of interest to declare.

Ethical approval and consent to participate
Not applicable.

Consent for publication
Not applicable.

Copyright

REFERENCES

1.   De, L. P.; Hahn, C.; Higgins, D.; et al. What would it take for renewably powered electrosynthesis to displace petrochemical processes? *Science* **2019**, *6438*, evva3506. DOI
2.   Rogelj, J.; den, E. M.; Hohne, N.; et al. Paris agreement climate proposals need a boost to keep warming well below 2 °C. *Nature* **2016**, *7609*, 631-9. DOI PubMed
3.   Shen, C.; Meng, X. Y.; Zou, R.; et al. Boosted sacrificial-agent-free selective photoreduction of CO_2 to CH_3OH by rhenium atomically dispersed on indium oxide. *Angew. Chem. Int. Ed. Engl.* **2024**, *63*, e202402369. DOI PubMed
4.   Ren, X.; Liu, F.; Wu, H.; et al. Reconstructed bismuth oxide through in situ carbonation by carbonate-containing electrolyte for

highly active electrocatalytic CO_2 reduction to formate. *Angew. Chem. Int. Ed. Engl.* **2024**, *63*, e202316640. DOI PubMed

5.   Liu, F.; Ren, X.; Zhao, J.; et al. Inhibiting sulfur dissolution and enhancing activity of sns for CO_2 electroreduction via electronic state modulation. *ACS. Catal.* **2022**, *12*, 13533-41. DOI

6.   Liu, F.; Wang, J.; Ren, X.; et al. In-situ reconstructed in doped SnO_2 amorphous-crystalline heterostructure for highly efficient CO_2 electroreduction with a dynamic structure-function relationship. *Appl. Catal. B-Environ.* **2024**, *352*, 124004. DOI

7.   Jiao, J.; Lin, R.; Liu, S.; Cheong, W. C.; Zhang, C.; et al. Copper atom-pair catalyst anchored on alloy nanowires for selective and efficient electrochemical reduction of CO_2. *Nat. Chem.* **2019**, *3*, 222-8. DOI

8.   Cai, Y.; Fu, J.; Zhou, Y.; et al. Insights on forming NO-coordinated Cu single-atom catalysts for electrochemical reduction CO_2 to methane. *Nat. Commun.* **2021**, *1*, 586. DOI PubMed PMC

9.   Zhang, T.; Li, W.; Huang, K. et al. Regulation of functional groups on graphene quantum dots directs selective CO_2 to CH_4 conversion. *Nat. Commun.* **2021**, *1*, 5265. DOI PubMed PMC

10.   Liu, X. C.; Wei, C.; Wu, Y.; et al. Tailoring the electrochemical protonation behavior of CO_2 by tuning surface noncovalent interactions. *ACS. Catalysis.* **2021**, *24*, 14986-94. DOI

11.   Zhang, Z.; Ahmad, F.; Zhao, W.; et al. Enhanced electrocatalytic reduction of CO_2 via chemical coupling between indium oxide and reduced graphene oxide. *Nano. Lett.* **2019**, *6*, 4029-34. DOI PubMed

12.   Zhao, Q.; Zhang, C.; Hu, R.; et al. Selective etching quaternary MAX phase toward single atom copper immobilized mxene ($Ti_3C_2Cl_x$) for efficient CO_2 electroreduction to methanol. *ACS. Nano.* **2021**, *3*, 4927-36. DOI

13.   Francke, R.; Schille, B.; Roemelt, M. Homogeneously catalyzed electroreduction of carbon dioxide - methods mechanisms and catalysts. *Chem. Rev.* **2018**, *9*, 4631-701. DOI PubMed

14.   Yin, Z.; Yu, C.; Zhao, Z. et al. *Nano. Lett.* **2019**, *12*, 8658-63. DOI

15.   Yin, J.; Gao, Z.; Wei, F.; et al. Customizable CO_2 electroreduction to C_1 or C_{2+} products through Cu_y/CeO_2 interface engineering. *ACS. Catalysis.* **2022**, *2*, 1004-11. DOI

16.   Gao, D.; Zegkinoglou, I.; Divins, N. J.; et al. Plasma-activated copper nanocube catalysts for efficient carbon dioxide electroreduction to hydrocarbons and alcohols. *ACS. Nano.* **2017**, *5*, 4825-31. DOI

17.   Ma, W.; Xie, S.; Liu, T.; et al. Electrocatalytic reduction of CO_2 to ethylene and ethanol through hydrogen-assisted C-C coupling over fluorine-modified copper. *Nature. Catalysis.* **2020**, *6*, 478-87. DOI

18.   Fan, L.; Xia, C.; Yang, F.; Wang, J.; Wang, H.; Lu, Y. Strategies in catalysts and electrolyzer design for electrochemical CO_2 reduction toward C_{2+} products. *Sci. Adv.* **2020**, *6*, eaay3111. DOI PubMed PMC

19.   Guzmán, H.; Russo, N.; Hernández, S. CO_2 valorisation towards alcohols by Cu-based electrocatalysts: challenges and perspectives. *Green. Chem.* **2021**, *5*, 1896-1920. DOI

20.   Nitopi, S.; Bertheussen, E.; Scott, S. B.; et al. Progress and perspectives of electrochemical CO_2 reduction on copper in aqueous electrolyte. *Chem. Rev.* **2019**, *12*, 7610-72. DOI

21.   Gu, J.; Hsu, C. S.; Bai, L.; Chen, H. M.; Hu, X. Atomically dispersed Fe^{3+} sites catalyze efficient CO_2 electroreduction to CO. *Science* **2019**, *364*, 1091-4. DOI PubMed

22.   Ross, M. B.; De, L. P.; Li, Y.; et al. Designing materials for electrochemical carbon dioxide recycling. *Nat. Catal.* **2019**, *8*, 648-58. DOI

23.   Singh, M. R.; Kwon, Y.; Lum, Y.; et al. Hydrolysis of electrolyte cations enhances the electrochemical reduction of CO_2 over Ag and Cu. *J. Am. Chem. Soc.* **2016**, *39*, 13006-12. DOI

24.   Huang, Y.; Ong, C. W.; Yeo, B. S. Effects of electrolyte anions on the reduction of carbon dioxide to ethylene and ethanol on copper (100) and (111) surfaces. *ChemSusChem* **2018**, *18*, 3299-306. DOI PubMed

25.   Kortlever, R.; Shen, J.; Schouten, K. J.; Calle-Vallejo, F.; Koper, M. T. Catalysts and reaction pathways for the electrochemical reduction of carbon dioxide. *J. Phys. Chem. Lett.* **2015**, *20*, 4073-82. DOI PubMed

26.   Benson, E. E.; Kubiak, C. P.; Sathrum, A. J.; Smieja, J. M. Electrocatalytic and homogeneous approaches to conversion of CO_2 to liquid fuels. *Chem. Soc. Rev.* **2009**, *1*, 89-99. DOI PubMed

27.   Zhang, H.; Ma, Y.; Quan, F.; et al. Selective electro-reduction of CO_2 to formate on nanostructured Bi from reduction of BiOCl nanosheets. *Electrochem. Commun.* **2014**, *46*, 63-6. DOI

28.   Zhang, J.; Lin, Q.; Wang, Z.; et al. Identifying water oxidation mechanisms at pure and titanium-doped hematite-based photoanodes with spectroelectrochemistry. *Small. Methods.* **2021**, *12*, e2100976. DOI

29.   Ricinschi, D.; Yun, K. Y.; Okuyama, M. A mechanism for the 150 μC cm^{-2} polarization of $BiFeO_3$ films based on first-principles calculations and new structural data. *J. Phys. Condens. Matter.* **2006**, *18*, L97. DOI PubMed

30.   Han, N.; Wang, Y.; Yang, H.; et al. Ultrathin bismuth nanosheets from in situ topotactic transformation for selective electrocatalytic CO_2 reduction to formate. *Nat. Commun.* **2018**, *1*, 1320. DOI PubMed PMC

31.   Yang, Z.; Oropeza, F. E.; Zhang, K. H. L. P-block metal-based (Sn In Bi Pb) electrocatalysts for selective reduction of CO_2 to formate. *APL. Materials.* **2020**, *6*, 060901. DOI

32.   Xiao, J.; Liu, S.; Sui, P. F.; et al. In-situ generated hydroxides realize near-unity CO selectivity for electrochemical CO_2 reduction. *Chem. Eng. J.* **2022**, *433*, 133785. DOI

33.   Komatsu, S.; Yanagihara, T.; Hiraga, Y.; Tanaka, M.; Kunugi, A. Electrochemical reduction of CO_2 at Sb and Bi electrodes in $KHCO_3$ solution. *Denki. Kagaku. oyobi. Kogyo. Butsuri. Kagaku.* **1995**, *3*, 217-224. DOI

34.   DiMeglio, J. L.; Rosenthal, J. Selective conversion of CO_2 to CO with high efficiency using an inexpensive bismuth-based

electrocatalyst. *J. Am. Chem. Soc.* **2013**, *24*, 8798-801. DOI PubMed PMC

35.   Medina-Ramos, J.; Pupillo, R. C.; Keane, T. P.; DiMeglio, J. L.; Rosenthal, J. Efficient conversion of CO_2 to CO using tin and other inexpensive and easily prepared post-transition metal catalysts. *J. Am. Chem. Soc.* **2015**, *15*, 5021-7. DOI PubMed

36.   Han, N.; Ding, P.; He, L.; Li, Y.; Li, Y. Promises of main group metal-based nanostructured materials for electrochemical CO_2 reduction to formate. *Adv. Energy. Mater.* **2019**, *11*, 201902338. DOI

37.   Li, P.; Yang, F.; Li, J.; et al. Nanoscale engineering of P-block metal-based catalysts toward industrial-scale electrochemical reduction of CO_2. *Adv. Energy. Mater.* **2023**, *34*, 202301597. DOI

38.   Guan, Y.; Liu, M.; Rao, X.; Liu, Y.; Zhang, J. Electrochemical reduction of carbon dioxide (CO_2): bismuth-based electrocatalysts. *J. Mater. Chem. A.* **2021**, *24*, 13770-803. DOI

39.   Xia, D.; Yu, H.; Xie, H.; et al. Recent progress of Bi-based electrocatalysts for electrocatalytic CO_2 reduction. *Nanoscale* **2022**, *22*, 7957-73. DOI

40.   Pan, F.; Yang, X.; O'Carroll, T.; et al. Carbon catalysts for electrochemical CO_2 reduction toward multicarbon products. *Adv. Energy. Mater.* **2022**, *24*, 202200586. DOI

41.   Koh, J. H.; Won, D. H.; Eom, T.; et al. Facile CO_2 electro-reduction to formate via oxygen bidentate intermediate stabilized by high-index planes of bi dendrite catalyst. *ACS. Catal.* **2017**, *8*, 5071-77. DOI

42.   Chen, J.; Tang, H.; Sun, Z.; Duan, L. Recent progress and challenges in heterogeneous CO_2 catalytic activation. *Curr. Opin. Green. Sust.* **2023**, *39*, 100720. DOI

43.   Bagger, A.; Ju, W.; Varela, A. S.; Strasser, P.; Rossmeisl, J. Electrochemical CO_2 reduction: a classification problem. *Chemphyschem* **2017**, *22*, 3266-73. DOI PubMed

44.   Jiang, H.; He, Q.; Zhang, Y.; Song, L. Structural self-reconstruction of catalysts in electrocatalysis. *Acc. Chem. Res.* **2018**, *11*, 2968-77. DOI

45.   Wang, F.; Li, Y.; Xia, X.; et al. Metal-CO_2 electrochemistry: from CO_2 recycling to energy storage. *Adv. Energy. Mater.* **2021**, *25*, 202100667. DOI

46.   Huang, J.; Hormann, N.; Oveisi, E.; et al. Potential-induced nanoclustering of metallic catalysts during electrochemical CO_2 reduction. *Nat. Commun.* **2018**, *1*, 3117. DOI PubMed PMC

47.   Kuznetsov, D. A.; Han, B.; Yu, Y.; et al. Tuning redox transitions via inductive effect in metal oxides and complexes and implications in oxygen electrocatalysis. *Joule* **2018**, *2*, 225-44. DOI

48.   De, L. P.; Quintero-Bermudez, R.; Dinh, C. T.; et al. Catalyst electro-redeposition controls morphology and oxidation state for selective carbon dioxide reduction. *Nature. Catalysis.* **2018**, *2*, 103-10. DOI

49.   Liu, X.; Meng, J.; Zhu, J.; et al. Comprehensive understandings into complete reconstruction of precatalysts: synthesis applications and characterizations. *Adv. Mater.* **2021**, *32*, e2007344. DOI

50.   Cao, C.; Ma, D. D.; Gu, J. F.; et al. Metal-organic layers leading to atomically thin bismuthene for efficient carbon dioxide electroreduction to liquid fuel. *Angew. Chem. Int. Ed. Engl.* **2020**, *35*, 15014-20. DOI PubMed

51.   Lamagni, P.; Miola, M.; Catalano, J.; et al. Restructuring metal-organic frameworks to nanoscale bismuth electrocatalysts for highly active and selective CO_2 reduction to formate. *Adv. Funct. Mater.* **2020**, *16;201910408*. DOI

52.   Wang, H.; Tong, Y.; Chen, P. Microenvironment regulation strategies of single-atom catalysts for advanced electrocatalytic CO_2 reduction to CO. *Nano. Energy.* **2023**, *118*, 108967. DOI

53.   Zhang, E.; Wang, T.; Yu, K.; et al. Bismuth single atoms resulting from transformation of metal-organic frameworks and their use as electrocatalysts for CO_2 reduction. *J. Am. Chem. Soc.* **2019**, *42*, 16569-73. DOI

54.   Santra, S.; Streibel, V.; Wagner, L. I.; et al. Tuning carbon dioxide reduction reaction selectivity of bi single-atom electrocatalysts with controlled coordination environments. *ChemSusChem* **2024**, *17*, e202301452. DOI PubMed

55.   Giannakakis, G.; Flytzani-Stephanopoulos, M.; Sykes, E. C. H. Single-atom alloys as a reductionist approach to the rational design of heterogeneous catalysts. *Acc. Chem. Res.* **2019**, *1*, 237-47. DOI

56.   Darby, M. T.; Stamatakis, M.; Michaelides, A.; Sykes, E. C. H. Lonely atoms with special gifts: breaking linear scaling relationships in heterogeneous catalysis with single-atom alloys. *J. Phys. Chem. Lett.* **2018**, *18*, 5636-46. DOI PubMed

57.   Greiner, M. T.; Jones, T. E.; Beeg, S.; et al. Free-atom-like d states in single-atom alloy catalysts. *Nat. Chem.* **2018**, *10*, 1008-15. DOI

58.   Sun, G.; Zhao, Z. J.; Mu, R.; et al. Breaking the scaling relationship via thermally stable Pt/Cu single atom alloys for catalytic dehydrogenation. *Nat. Commun.* **2018**, *1*, 4454. DOI PubMed PMC

59.   Cao, Y.; Chen, S.; Bo, S.; et al. Single atom bi decorated copper alloy enables C-C coupling for electrocatalytic reduction of CO_2 into C_{2+} Products. *Angew. Chem. Int. Ed. Engl.* **2023**, *30*, e202303048. DOI

60.   Fan, K.; Jia, Y.; Ji, Y.; et al. Curved surface boosts electrochemical CO_2 reduction to formate via bismuth nanotubes in a wide potential window. *ACS. Catalysis.* **2019**, *1*, 358-64. DOI

61.   Guan, A.; Yang, C.; Quan, Y.; et al. One-dimensional nanomaterial electrocatalysts for CO_2 Fixation. *Chem. Asian. J.* **2019**, *22*, 3969-80. DOI

62.   Zhang, X.; Sun, X.; Guo, S. X.; Bond, A. M.; Zhang, J. Formation of lattice-dislocated bismuth nanowires on copper foam for enhanced electrocatalytic CO_2 reduction at low overpotential. *Energ. Environ. Sci.* **2019**, *4*, 1334-40. DOI

63.   Zhang, W.; Hu, Y.; Ma, L.; et al. Liquid-phase exfoliated ultrathin Bi nanosheets: uncovering the origins of enhanced electrocatalytic CO_2 reduction on two-dimensional metal nanostructure. *Nano. Energy.* **2018**, *53*, 808-16. DOI

64.   Hu, Y.; Liang, J.; Gu, Y.; et al. Sandwiched epitaxy growth of 2D single-crystalline hexagonal bismuthene nanoflakes for electrocatalytic CO_2 reduction. *Nano. Letters.* **2023**, *22*, 10512-21. DOI

65.   Feng, X.; Zou, H.; Zheng, R.; et al. Bi_2O_3/BiO_2 nanoheterojunction for highly efficient electrocatalytic CO_2 reduction to formate. *Nano. Lett.* **2022**, *4*, 1656-64. DOI

66.   Tian, J.; Wang, R.; Shen, M.; et al. Bi-Sn oxides for highly selective CO_2 electroreduction to formate in a wide potential window. *ChemSusChem* **2021**, *10*, 2247-54. DOI

67.   Gong, Q.; Ding, P.; Xu, M.; et al. Structural defects on converted bismuth oxide nanotubes enable highly active electrocatalysis of carbon dioxide reduction. *Nat. Commun.* **2019**, *1*, 2807. DOI PubMed PMC

68.   Yang, S.; Jiang, M.; Zhang, W.; et al. In situ structure refactoring of bismuth nanoflowers for highly selective electrochemical reduction of CO_2 to formate. *Adv. Funct. Mater.* **2023**, *37*, 202301984. DOI

69.   Tran-Phu, T.; Daiyan, R.; Fusco, Z.; et al. Nanostructured β-Bi_2O_3 fractals on carbon fibers for highly selective CO_2 electroreduction to formate. *Adv. Funct. Mater.* **2019**, *3*, 201906478. DOI

70.   Liu, S.; Lu, X. F.; Xiao, J.; et al. Bi_2O_3 nanosheets grown on multi-channel carbon matrix to catalyze efficient CO_2 electroreduction to HCOOH. *Angew. Chem. Int. Ed. Engl.* **2019**, *39*, 13828-33. DOI

71.   Ye, K.; Zhou, Z.; Shao, J.; et al. In situ reconstruction of a hierarchical Sn-Cu/SnOx core/shell catalyst for high-performance CO_2 electroreduction. *Angew. Chem. Int. Ed. Engl.* **2020**, *12*, 4814-21. DOI

72.   Das, S.; Perez-Ramirez, J.; Gong, J.; et al. Core-shell structured catalysts for thermocatalytic photocatalytic and electrocatalytic conversion of CO_2. *Chem. Soc. Rev.* **2020**, *10*, 2937-3004. DOI

73.   Zhao, Y.; Liu, X.; Liu, Z.; et al. Spontaneously Sn-doped Bi/BiOx core-shell nanowires toward high-performance CO_2 electroreduction to liquid fuel. *Nano. Lett.* **2021**, *16*, 6907-13. DOI

74.   Zhang, Y.; Zhang, X.; Ling, Y.; et al. Controllable synthesis of few-layer bismuth subcarbonate by electrochemical exfoliation for enhanced CO_2 reduction performance. *Angew. Chem. Int. Ed. Engl.* **2018**, *40*, 13283-87. DOI

75.   Lv, W.; Bei, J.; Zhang, R.; et al. $Bi_2O_2CO_3$ nanosheets as electrocatalysts for selective reduction of CO_2 to formate at low overpotential. *ACS. Omega.* **2017**, *6*, 2561-7. DOI PubMed PMC

76.   Wang, Y.; Wang, B.; Jiang, W.; et al. Sub-2 nm ultra-thin $Bi_2O_2CO_3$ nanosheets with abundant Bi-O structures toward formic acid electrosynthesis over a wide potential window. *Nano. Research.* **2021**, *4*, 2919-27. DOI

77.   Fu, H. Q.; Liu, J.; Bedford, N. M.; et al. Operando converting BiOCl into $Bi_2O_2(CO_3)_xCl_y$ for efficient electrocatalytic reduction of carbon dioxide to formate. *Nanomicro. Lett.* **2022**, *1*, 121. DOI PubMed PMC

78.   Wu, M.; Xiong, Y.; Hu, B.; et al. Indium doped bismuth subcarbonate nanosheets for efficient electrochemical reduction of carbon dioxide to formate in a wide potential window. *J. Colloid. Interface. Sci.* **2022**, *624*, 261-9. DOI

79.   Lv, L.; Lu, R.; Zhu, J.; et al. Coordinating the edge defects of bismuth with sulfur for enhanced CO_2 electroreduction to formate. *Angew. Chem. Int. Ed. Engl.* **2023**, *25*, e202303117. DOI

80.   Wang, Z.; Wang, C.; Hu, Y.; et al. Simultaneous diffusion of cation and anion to access N S co-coordinated Bi-sites for enhanced CO_2 electroreduction. *Nano. Research.* **2021**, *8*, 2790-6. DOI

81.   Luo, Y.; Chen, S.; Zhang, J.; et al. Perovskite-derived bismuth with I^- and Cs^+ dual modification for high-efficiency CO_2 -to-formate electrosynthesis and Al-CO_2 batteries. *Adv. Mater.* **2023**, *36*, e2303297. DOI

82.   Yang, S.; An, H.; Arnouts, S.; et al. Halide-guided active site exposure in bismuth electrocatalysts for selective CO_2 conversion into formic acid. *Nature. Catalysis.* **2023**, *9*, 796-806. DOI

83.   Wang, D.; Wang, Y.; Chang, K.; et al. Residual iodine on in situ transformed bismuth nanosheets induced activity difference in CO_2 electroreduction. *J. CO2. Utili.* **2022**, *55*, 101802. DOI

84.   Li, Y.; Chen, J.; Chen, S.; et al. In situ confined growth of bismuth nanoribbons with active and robust edge sites for boosted CO_2 electroreduction. *ACS. Energy. Letters.* **2022**, *4*, 1454-61. DOI

85.   Zhao, S.; Qin, Y.; Wang, X.; et al. Anion exchange facilitates the in situ construction of Bi/Bi-O interfaces for enhanced electrochemical CO_2 -to-formate conversion over a wide potential window. *Small* **2023**, *43*, e2302878. DOI

86.   Liu, S.; Fan, Y.; Wang, Y.; et al. Surface-oxygen-rich Bi@C nanoparticles for high-efficiency electroreduction of CO_2 to formate. *Nano. Lett.* **2022**, *22*, 9107-14. DOI

87.   Liu, S.; Hu, B.; Zhao, J.; et al. Enhanced electrocatalytic CO_2 reduction of bismuth nanosheets with introducing surface bismuth subcarbonate. *Coatings* **2022**, *2*, 12020233. DOI

88.   Li, J. F.; Huang, Y. F.; Ding, Y.; et al. Shell-isolated nanoparticle-enhanced raman spectroscopy. *Nature* **2010**, *7287*, 392-5. DOI

89.   Sui, P. F.; Gao, M. R.; Liu, S.; et al. Carbon dioxide valorization via formate electrosynthesis in a wide potential window. *Adv. Funct. Mater.* **2022**, *32*, 202203794. DOI

90.   Cui, R.; Yuan, Q.; Zhang, C.; et al. Revealing the behavior of interfacial water in te-doped bi via operando infrared spectroscopy for improving electrochemical CO_2 reduction. *ACS. Catalysis.* **2022**, *18*, 11294-300. DOI

91.   Li, J.; Li, J.; Liu, X.; et al. Probing the role of surface hydroxyls for Bi Sn and In catalysts during CO_2 Reduction. *Appl. Catal. B. Environ.* **2021**, *298*, 120581. DOI

92.   Zhang, H.; Liang, Z.; Huang, C.; et al. Enhanced dissociation activation of CO_2 on the Bi/Cu(111) interface by the synergistic effect. *J. Catal.* **2022**, *410*, 1-9. DOI

93.   Jiang, X.; Lin, L.; Rong, Y.; et al. Boosting CO_2 electroreduction to formate via bismuth oxide clusters. *Nano. Res.* **2022**, *10*, 12050-57. DOI

94.   Xiao, L.; Wang, G.; Huang, X.; et al. Efficient CO_2 reduction MOFs derivatives transformation mechanism revealed by in situ liquid phase TEM. *Appl. Catal. B-Environ.* **2022**, *307*, 121164. DOI

95.   Dong, J.; Chen, J.; Wang, W.; et al. Charged microdroplets as microelectrochemical cells for CO_2 reduction and C-C coupling. *J. Am. Chem. Soc.* **2024**, *146*, 2227-36. DOI

96.   Wang, Z. Y.; He, Z. H.; Li, L. Y.; et al. Research progress of CO_2 oxidative dehydrogenation of propane to propylene over Cr-free metal catalysts. *Rare. Metals.* **2022**, *41*, 2129-52. DOI PubMed PMC

97.   Jiang, Y.; Xie, H.; Han, L.; et al. Advances in TiS_2 for energy storage, electronic devices, and catalysis: a review. *Prog. Nat. Sci-Mater.* **2023**, *33*, 133-50. DOI

98.   Ju, L.; Tang, X.; Kou, L. Polarization boosted catalysis: progress and outlook. *Microstructures* **2022**, *2*, 2022008. DOI

99.   Wang, J.; Zhang, Z.; Ding, J. Recent progresses of micro-nanostructured transition metal compound-based electrocatalysts for energy conversion technologies. *Sci. China. Mater.* **2021**, *64*, 1-26. DOI

100.   Wang, J.; Li, X.; Cui, B.; et al. A review of non-noble metal-based electrocatalysts for CO_2 electroreduction. *Rare. Met.* **2021**, *40*, 3019-303. DOI

101.   Hu, Q.; Chen, Z.; Wang, J. Nanoporous nickel with rich adsorbed oxygen for efficient alkaline hydrogen evolution electrocatalysis. *Sci. China. Mater.* **2022**, *65*, 1825-32. DOI

102.   Huang, B.; Sun, Z.; Sun, G. Recent progress in cathodic reduction-enabled organic electrosynthesis: trends, challenges, and opportunities. *eScience* **2022**, *2*, 243-77. DOI

103.   Rabinowitz, J. A.; Kanan, M. W. The future of low-temperature carbon dioxide electrolysis depends on solving one basic problem. *Nat. Commun.* **2020**, *11*, 5231. DOI PubMed PMC

104.   Higgins, D.; Hahn, C.; Xiang, C.; Jaramillo, T. F.; Weber, A. Z. Gas-diffusion electrode for carbon dioxide reduction: a new paradigm. *ACS. Energy. Letters.* **2019**, *4*, 317-24. DOI PubMed

105.   Pan, B.; Fan, J.; Zhang, J.; et al. Close to 90% single-pass conversion efficiency for CO_2 electroreduction in an acid-fed membrane electrode assembly. *ACS. Energy. Lett.* **2022**, *7*, 4224-31,. DOI

106.   Chi, L. P.; Niu, Z. Z.; Zhang, Y. C.; et al. Efficient and stable acidic CO_2 electrolysis to formic acid by a reservoir structure design. *P. Natl. Acad. Sci. Usa.* **2023**, *120*, e2312876120. DOI PubMed PMC